NANOFIBROUS SCAFFOLD FOR BURN WOUND HEALING AND REGENERATION

A DISSERTATION

Submitted in partial fulfilment of the

requirements for the award of the degree

of

MASTER OF TECHNOLOGY

in

NANOTECHNOLOGY

By

ISHA GOEL

(17551003)

CENTRE OF NANOTECHNOLOGY
INDIAN INSTITUTE OF TECHNOLOGY ROORKEE
ROORKEE - 247667 (INDIA)
JUNE, 2019

NANOFIBEROUS SCAFFOLD FOR BURN WOUND HEALING AND REGENERATION

A DISSERTATION

Submitted in partial fulfilment of the
requirements for the award of the degree

of

MASTER OF TECHNOLOGY

in

NANOTECHNOLOGY

Under the supervision of

Dr. Debrupa Lahiri
Associate Professor
Department of Metallurgical
and Materials Engineering,
I.I.T. Roorkee

Dr. Partha Roy
Professor
Department of Biotechnology
I.I.T. Roorkee

Submitted by
Isha Goel (17551003)

CENTRE OF NANOTECHNOLOGY

INDIAN INSTITUTE OF TECHNOLOGY ROORKEE

ROORKEE-247667

JUNE, 2019

CANDIDATE'S DECLARATION

I hereby declare that the work presented in the dissertation entitled **"NANOFIBROUS SCAFFOLD FOR BURN WOUND HEALING AND REGENERATION"** submitted in partial fulfilment of the requirement for the award of degree of **Master of Technology** in **Nanotechnology, Indian Institute of Technology Roorkee,** is an authentic record of my own work carried out under the supervision of **Dr. Partha Roy**, Professor, Department of Biotechnology, I.I.T. Roorkee and **Dr. Debrupa Lahiri,** Associate Professor, Department of Metallurgical and Materials Engineering, I.I.T. Roorkee.

The matter presented in this dissertation has not been submitted by me for the award of any other degree of this or any other institution.

(Isha Goel)

Enrolment No. 17551003

Date:

CERTIFICATE

This is to certify that the above statement made by the candidate is correct to the best of my knowledge.

(Dr. Partha Roy)

Supervisor
Professor
Dept. of Biotechnology
I.I.T. Roorkee

(Dr. Debrupa Lahiri)

Supervisor
Associate Professor
Dept. of Metallurgical and
Materials Engineering
I.I.T. Roorkee

TO WHOM SO EVER IT MAY CONCERN

It is hereby declared that the work presented in the dissertation entitled **"NANOFIBROUS SCAFFOLD FOR BURNT-WOUND HEALING AND REGENERATION"** submitted in partial fulfilment of the requirement for the award of the degree of Master of Technology in Nanotechnology, Indian Institute of Technology Roorkee is **CONFIDENTIAL**. The patent for the work has been applied for, through the Head of Department, Centre of Nanotechnology (CON) to the Intellectual Property Right (IPR) cell Indian Institute of Technology (IITR). **The Intellectual Property Right (IPR) of the work is with I.I.T. Roorkee.**

(Dr. Partha Roy)	**(Dr. Debrupa Lahiri)**	**(Dr. R. K. Dutta)**
Supervisor	Supervisor	H. O. D.
Professor	Associate Professor	Centre of
Dept. of Biotechnology	Dept. of Metallurgical and	Nanotechnology
I.I.T. Roorkee	Materials Engineering	I.I.T. Roorkee
	I.I.T. Roorkee	

(Isha Goel)

Student
M.Tech Nanotechnology
Centre of Nanotechnology
I.I.T. Roorkee

Acknowledgement

I am very grateful to my mentors, **Dr. Debrupa Lahiri,** Associate Professor, Department of Metallurgical and Materials Engineering, I.I.T. Roorkee and **Dr. Partha Roy,** Professor, Department of Biotechnology, I.I.T. Roorkee**.** Their expertise, understanding and generous guidance made it possible for me to work on a topic that was of great interest to me and to persevere and complete it satisfactorily. Without their ingenious suggestions, assistance, care and security, this research work would not have taken its present shape. It has indeed been an enriching scientific experience and I thank them for providing me with this opportunity and guidance in all time of research and writing of this thesis. I could not have imagined having better advisors and mentors for my study.

I thank **M.H.R.D.** for supporting my master's program. I would like to offer my gratitude to the Head of the Centre of Nanotechnology, **Dr. R. K. Dutta** for providing me with the best resources. I thank **Dr. Indranil Lahiri** for his faith, support, kind advises and all-time access to facilities for my work. I am very grateful.

I owe huge and very special thanks to Post-Doctoral Fellow, **Dr. Swati Haldar** of the Centre of Nanotechnology at I.I.T. Roorkee. The door to Dr. Haldar's office was always open, day or night, whenever I ran into a trouble spot or had a question about my research or writing. She consistently allowed me to expand the horizons of my thinking but steered me in the right direction whenever she thought I needed it. She allowed me to work as a team with her with equal contribution in all decisions. Without her passionate participation, companionship and input, the research project could not have been successfully conducted.

I am gratefully indebted to my lab seniors **Mr. Viney Kumar Jhakhard** and **Mr. Souvik Ghosh** during the period of this work for their very valuable comments on this thesis. The hand holding support, continuous presence and invigorating environment created by them becomes a driving force in itself. They can make a stressful journey a happy walk. They hold huge contribution in all *in vitro* and *in vivo* studies.

In the later work of *in vivo* confirmation, I am particularly indebted to our collaborators from Dept. of Pharmacology, M.M. University, Mullana **Dr. Sumeet Gupta** (Dean and Principal), **Mr. Samrat Chauhan** (Assistant Professor), **Mr. Saahil, Mr. Arif** and **Mr. Abhishek Kumar** (Masters students). I highly appreciate their collaboration and impressive skills. Their interest, meticulous experimental skills and helpful discussions made the study confirmations a smooth feat.

Special thanks to **Mr. Narasimha Vinod Pulagara, Mr. Shanid Mohiyuddin, Mr. Vinay Kumar** and **Mr. Palash Chandra Maity** for sharing their precious time and technical expertise. My, Biomaterials and Multiscale Mechanics group seniors **Mr. Siddharth Sharma, Ms. Ankita Bisht, Ms. Anshu Dubey, Mr. Satish Jaiswal, Mr. Vaibhav Jain, Mr. Kanike Rajesh** and **Mr. Pradeep Singh Thakur**; Nanomaterials & Applications Lab group seniors **Ms. Gurjinder Kaur, Mr. Narasimha Vinod Pulagara, Mr. Palash Chandra Maity, Ms. Akanksha R. Urade** and **Mr. Atif Suhail**; and my Molecular Endocrinology group seniors **Mr. Somesh Banerjee, Ms. Rutu Mishra, Mr. Niladri Das, Ms. Parul Katiyar, Mr. Sandeep Nathani** and **Ms. Sakshi Saini** provided an ever friendly atmosphere and help whenever needed. I am eternally grateful to be a part of these groups.

I would extend my thanks to non-technical staff **Mr. Ravan Pal** and team of Centre of Nanotechnology for their endless support. I also thank technical staff **Mr. D Prasad, Mr. Shiv Kumar** and **Mr. Gautam** and non-technical staff IIC (Institute Instrumentation Centre) for their invaluable help. My hearty thanks to **Mr. D.C. Meena**, Tech. Officer and **Mr. Madan Pal**, Y-Pool Worker, Department of Chemistry for their patience and technical support.

My friends and batchmates along with my parents have been the most gracious and understanding. Thanks for cheering me up always.

(Isha Goel)

Student M. Tech Nanotechnology
Centre of Nanotechnology, I.I.T. Roorkee

<u>Abstract</u>

Burns, unlike other wounds, show high variability in terms of tissue affected, severity and resultant fatal complications including shock, infection, electrolyte imbalances and spectrum of complex inflammatory response reactions. Following complete epithelialization, the remodeling phase is prolonged, and may take years for scar maturation. Infection adds significant complication to burns due to damaged structural and mechanical integrity of the skin and generalized immune suppression. Moist, protein-rich avascular eschar or blister that encourages microbial growth, replaces the skin barrier. Hampered migration of immune cells and release of intermediaries, impede the immune response. Eschar also restricts distribution of systemically administered antibiotics.

Scope of improvisation lies in burn wound management efficiency and developing a more economical system for topical care catering to pain- and scar-less healing. The present work aims to resolve the situation by developing a multilayer biopolymer scaffold fortified with antibiotics and bioactive agent focusing on full thickness burn wounds. The biopolymer layers are meticulously assembled to support skin cell migration and proliferation by providing the right microenvironment. Wound moisture control and exudate management are taken care by a hydrophobicity variation across the depth of the scaffold. The presence of antibiotics and bioactive agent will facilitate protection from infections and expedite healing, respectively. The scaffold serves as an extracellular matrix for regeneration of the destroyed tissue, tuned in detail to serve towards scar and contracture free healing. This biodegradable scaffold will be the first of its kind to address agonizing repeated replacement of bandages thereby, ensuring less painful healing of full thickness burn wounds. A functional blend of natural and synthetic components is proposed as prospective answer for efficient management of second and third degree burn wounds economically.
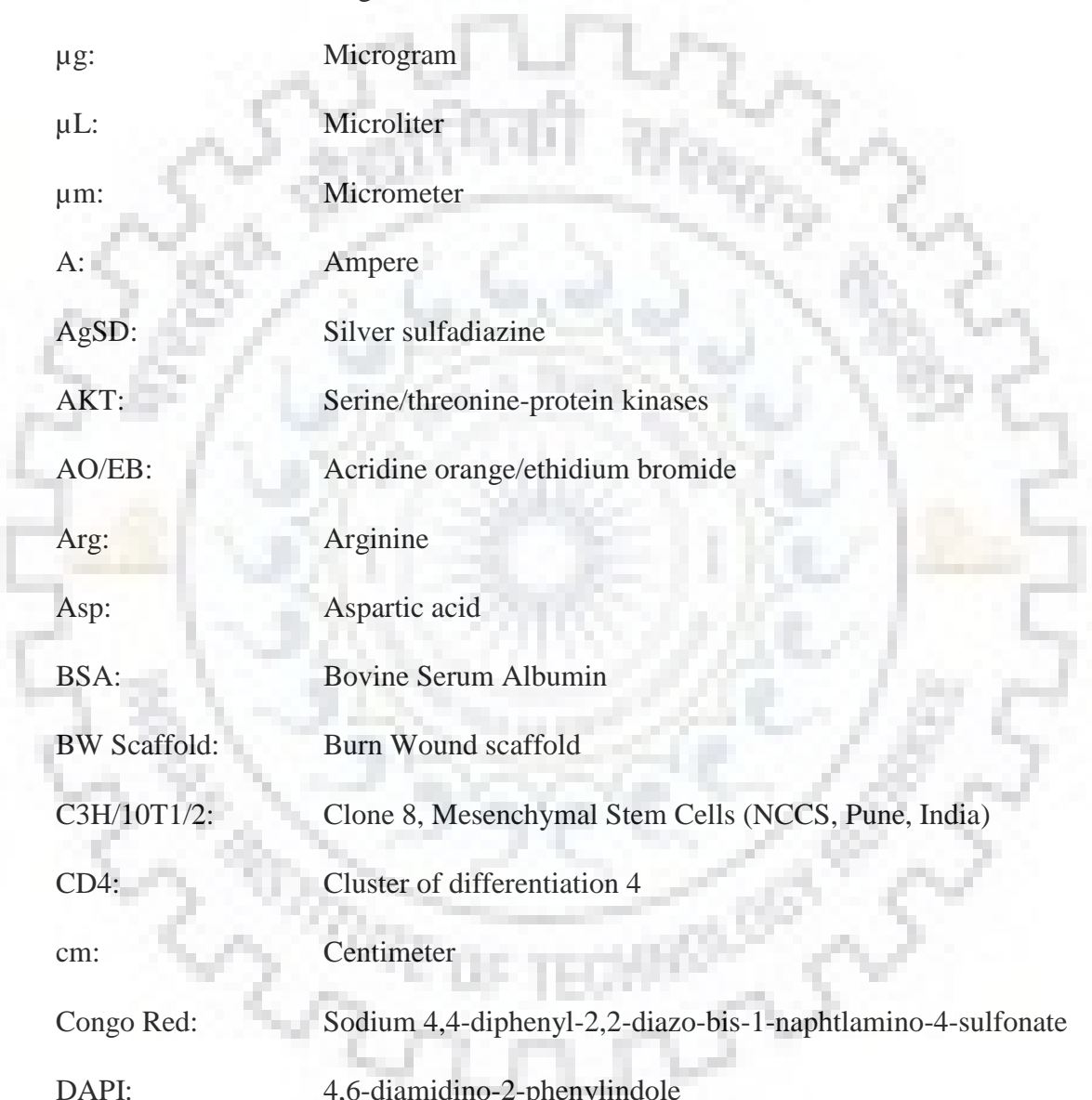
Key words: Third degree burn wounds, trilayer scaffold, biodegradable, biopolymer, antibiotics and anti-inflammatory agent.
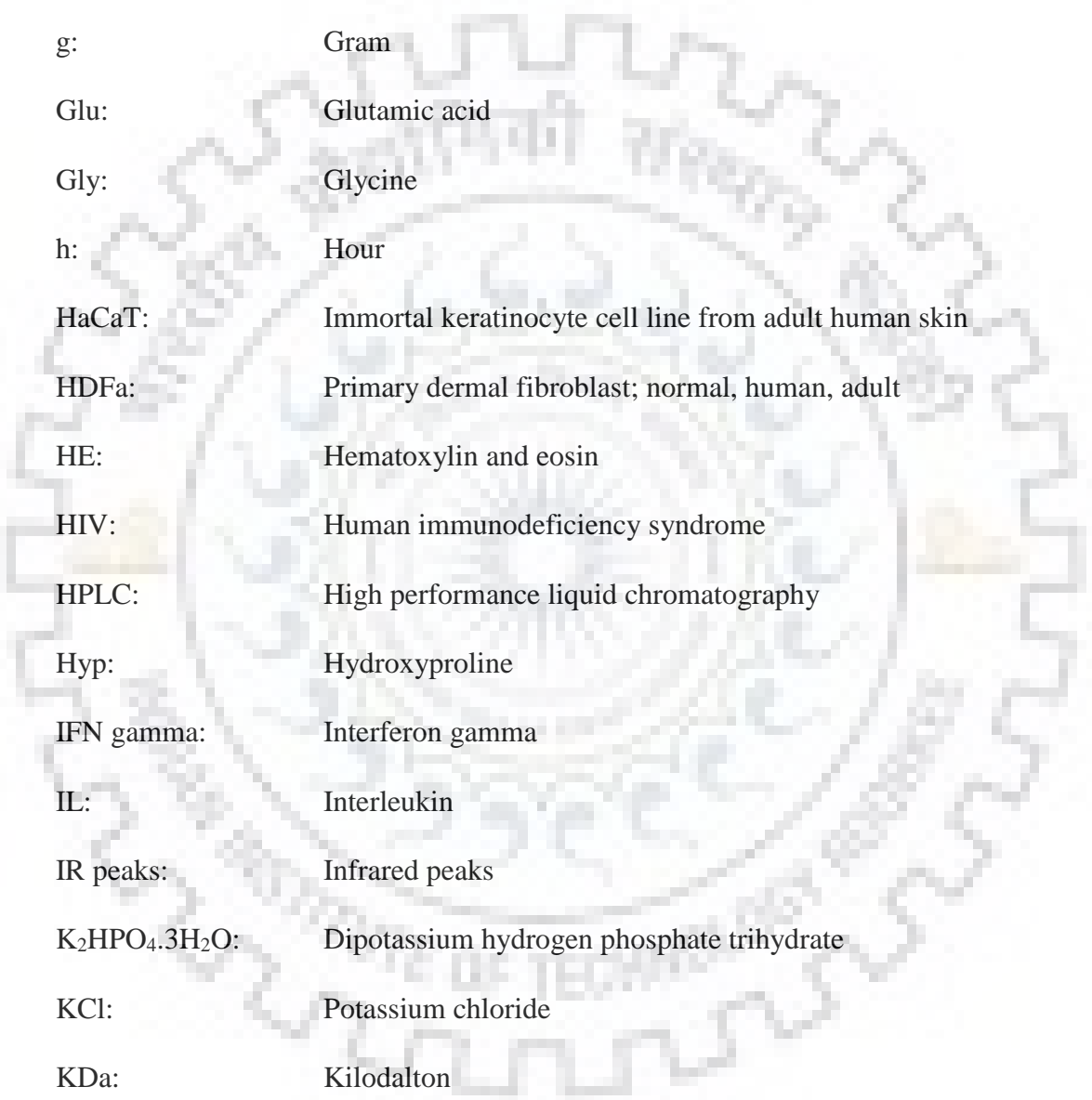
Contents

List of Abbreviations

®:	Registered trademark symbol
°C:	Degree Celsius
μg:	Microgram
μL:	Microliter
μm:	Micrometer
A:	Ampere
AgSD:	Silver sulfadiazine
AKT:	Serine/threonine-protein kinases
AO/EB:	Acridine orange/ethidium bromide
Arg:	Arginine
Asp:	Aspartic acid
BSA:	Bovine Serum Albumin
BW Scaffold:	Burn Wound scaffold
C3H/10T1/2:	Clone 8, Mesenchymal Stem Cells (NCCS, Pune, India)
CD4:	Cluster of differentiation 4
cm:	Centimeter
Congo Red:	Sodium 4,4-diphenyl-2,2-diazo-bis-1-naphtlamino-4-sulfonate
DAPI:	4,6-diamidino-2-phenylindole
DMEM:	Dulbecco's minimum essential medium
DMSO:	Dimethyl sulphoxide
DPX:	Mixture of distyrene, a plasticizer and xylene

E.coli:	*Escherichia coli*
ECM:	Extracellular matrix
FESEM:	Field Emission Scanning Electron Microscope
FITC conjugated:	Fluorescein iso-thiocyanate
g:	Gram
Glu:	Glutamic acid
Gly:	Glycine
h:	Hour
HaCaT:	Immortal keratinocyte cell line from adult human skin
HDFa:	Primary dermal fibroblast; normal, human, adult
HE:	Hematoxylin and eosin
HIV:	Human immunodeficiency syndrome
HPLC:	High performance liquid chromatography
Hyp:	Hydroxyproline
IFN gamma:	Interferon gamma
IL:	Interleukin
IR peaks:	Infrared peaks
$K_2HPO_4.3H_2O$:	Dipotassium hydrogen phosphate trihydrate
KCl:	Potassium chloride
KDa:	Kilodalton
kV:	Kilovolt
L:	Liter
LB:	Luria Bertani

LR:	Laboratory grade
M:	Molarity
mg:	milligram
$MgCl_2.6H_2O$:	Magnesium chloride hexahydrate
MHC:	Major histocompatibility complex
mL:	Milli Liter
mm:	Milli meter
MMP:	Matrix metalloproteinases
MPa:	Megapascal
MTCC:	Microbial type cell culture
mTOR :	Mechanistic target of rapamycin
MTT:	3-(4,5-Dimethylthiazol-2-yl)-2,5-Diphenyltetrazolium Bromide
N:	Normality
NA:	Nutrient agar
Na_2HPO_4:	Disodium hydrogen phosphate
Na_2SO_4:	Sodium Sulphate
NaCl:	Sodium Chloride
NaOH:	Sodium Hydroxide
NB:	Nutrient broth
NBF:	Neutral buffered formalin
NBF:	Normal Buffered Saline
NCCS:	National Centre for Cell Science
nm:	Nanometer

PBS: Phosphate Buffered Saline

PCL: Polycaprolactone

Phe: Phenylalanine

rpm: Revolution per minute

S.aureus: *Staphylococcus aureus*

SBWE: Simulated Burn Wound Exudate

SE: Standard Error

SGOT: Serum glutamic-oxaloacetic transaminase

SGPT: Serum glutamic pyruvic transaminase

SRL: Sisco Research Laboratories Pvt. Ltd.

TBSA: Total body surface area

TEM: Transmission electron microscopy

TLC: Total leukocyte count

UTS: Ultimate Tensile Strength

UV: Ultraviolet

w/v: Weight by volume

W_f: Dry weight at specific time point

W_i: Initial dry weight

W_s: Wet weight at specific time point

ZO-1:   *Zona occludens*

α-MEM: Minimum essential medium eagle alpha

List of figures

List of tables

1.   Introduction

Every year an estimated 1,80,000 deaths are caused by burns, majorly in low- and middle-income countries. Non-fatal burns are a leading cause of morbidity, including prolonged hospitalization, disfigurement and disability, often with resulting stigma and rejection. Around 11 million people worldwide required medical attention due to burn injuries in 2004[1].

Burn injury is a complex traumatic event with various local and systemic effects, affecting several organ systems beyond the skin. Unlike other wounds they are characterised by high variability in terms of tissue affected, severity and resultant fatal complications including shock, infection, electrolyte imbalances and spectrum of complex inflammatory response reactions. Even after complete epithelization, the remodelling phase is prolonged, and might take years for scar maturation. Infections are significant complication of burn wounds. Infections are highly probable due to disruption of the skin's integrity and generalised immune suppression. Eschar or blister replaces the skin barrier[2]. This moist, protein-rich avascular environment encourages microbial growth. Hampered migration of immune cells and release of intermediaries, impede the immune response. Eschar also restricts distribution of systemically administered antibiotics because of its avascularity[3].

Scope of improvisation lies in burn wound management efficiency and developing a more economical system for topical care catering to pain- and scar-less healing. The present work aims to resolve the situation by developing a multilayer biopolymer scaffold fortified with antibiotic and regenerative agent focusing on full thickness burn wounds. The biopolymer layers are minutely assembled to support skin cell migration and proliferation by providing the right micro environment. Exudate management and wound moisture control are catered to by maintaining a porosity gradient and absorbing excess exudate. The presence of antibiotic and regenerative agent will facilitate at the door protection from infections and faster healing respectively. The presence of scaffold serves as extracellular matrix for the destroyed tissue, tuned in detail can serve towards scar and

contracture free healing. This biodegradable scaffold will be an excellent alternative to the agonizing repeated replacement of bandages thereby, ensuring painless healing.

The scaffold composition comprises of three layers. The scaffold is an amalgamation of various fabrication techniques. Layer 1, the top outer most layer, is a non-porous layer, followed by layer 2 incorporated with antibiotics and regenerative agent. Layer 3 is incorporated with regenerative agent. The schematic of working of **BW** (**B**urn **W**ound) scaffold is presented in **Figure 1**.
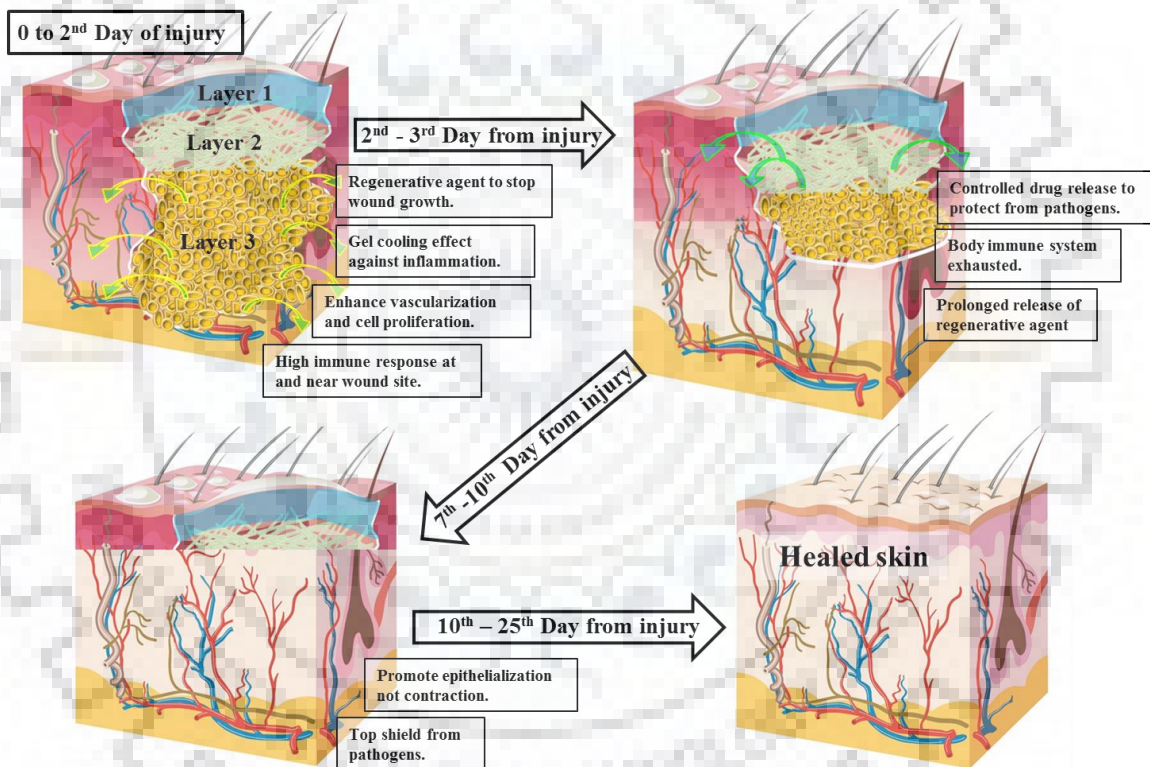
Figure 1: Representative schematic of working of BW scaffold in burn wound healing.

2. Literature Review

Burn wounds are among the most difficult ones to be treated. Extent of tissue damage depends on the degree of burn caused. In case of second-degree burns, epidermis and part of dermis are damaged. This damage extends through full thickness of dermis and sometimes beyond in case of third- degree burn wounds. Severity of these wounds is significantly raised due to high risks of bacterial infection. Gross absence of functional blood vessels due to severe charring in case of second- and third-degree burns, makes effective intra-venous administration of antibiotics almost impossible. Burn wounds require treatment at different levels: debridement, decontamination, vascularization and tissue reconstruction.

2.1.   Biology of burn wounds

Skin is composed of different layers, top covering that completes wound healing is epidermis while the following layer that gives strength and stability is dermis. Epidermis hold the ability of complete regeneration and forms replica of original in case of burns limited to the epidermis. The junction between epidermis and dermis holds epidermal papillary structures which too have the properties of regeneration and repair. Dermis devoid of these epidermal structures has no regenerative properties and is called reticular dermis. Burns and wounds reaching the deep dermis, are healed via swift contraction or reparative process leading to formation of deformation or hypertrophic scars (**Figure 2a**).

Burn wounds are classified as first-, second-, third- and fourth-degree wounds according to their depth and severity (**Figure 2**).

➢ **First degree burns** account only for redness (erythema), a white plaque and minor pain at the site of injury. These burns involve only the epidermis and heal in 3 -5 days without scarring (**Figure 2b**).

➢ **Second-degree burns** are divided into two categories superficial and deep. Superficial dermis burns have erythema along with superficial blistering of the skin, involving the epidermis and superficial (papillary) dermis. They heal in 10 -20 days

with minimal scarring (**Figure 2c**). Deep dermis burns involve the deep (reticular) dermis layer and the wound are elastic, soft and waxy white. They heal in 3 to 5 weeks and cause hypertrophic scars (**Figure 2d**).

➢ **Third-degree burns** are characterized by the loss of epidermis and damage reaching till the subcutaneous tissue. Burn wounds exhibit charring and hard parchment like eschar is formed. (**Figure 2e**).

➢ **Fourth degree burns** represent damage reaching the muscle, tendon, and ligament tissues, resulting in charring and drastic damage to the subcutaneous tissue.

Burns are also assessed in terms of total body surface area (%TBSA), which is the percentage affected by partial thickness or full thickness burns
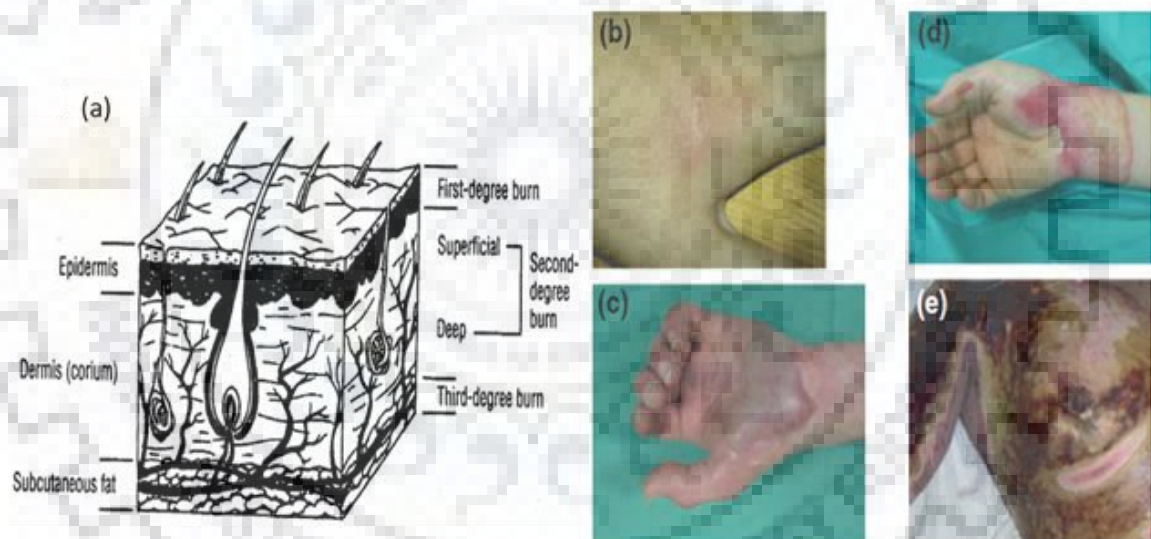
Figure 2: Classification of burn wound depth. **(a)** histologic overview[4], **(b–e)** clinical examples of burn degrees[2]; (b) superficial first degree, (c) superficial dermal second degree, (d) deep partial second degree, (e) full thickness third degree.

The area of severe burn wounds is divided into three zones (**Figure 3**), the central most affected being zone of coagulation, which has totally lost regenerative ability and is whitish is appearance. Then is zone of stasis which is light pink in appearance and can

regenerate with external support and favorable conditions. The outer most is zone of hyperaemia, which still has regenerative ability and can heal with the support of bordering normal cells present. Severely burned skin loses ability to act as barrier against water loss and bacterial invasion. Proinflammatory cascade is activated following the injury, which plays a role in development of immune dysfunction, susceptibility to sepsis and multiple organ failure.

Burn wounds are dynamic in nature. As the local response to injury not only includes tissue coagulation but also conversion[5]. Where the damaged cells initiate apoptosis and necrosis in turn extending the depth and severity of the wound. Deep burn wounds reach their peak in approximately 3 days. The massive release of proinflammatory cytokines, chemical mediator and immune defensins due to the shock faced by the system, leads to an acute shortage in availability of immune mediators[3]. The surge of degranulation leaves the immune system impaired with an inability to replenish and susceptible to infections. Hence the wounds are sterile initially due to extensive degranulation but later very susceptible to infections and sepsis. Damaged vascular system at wound site lead to lack of delivery system in the immunocompromised state[2].

Figure 3: Scald burn in a child showing the Jackson's three zones of damage i.e., **(a)** Zone of coagulation, **(b)** Zone of stasis, **(c)** Zone of hyperaemia[6].

Thermal damage destroys the microvasculature making burn a non-vascularized tissue. Proteolysis and lipolysis are upregulated. For instance, there is a marked increase in matrix metalloproteinases aimed for breakdown of protein for remodeling phase of healing, but also leads to provide more nutrients for microbes and makes microbial penetration into the tissue easier[7]. Initially the immune response is proinflammatory in nature but later becomes anti-inflammatory to help restore normal physiology and maintain homeostasis. Adaptive immunity consisting of B and T cells are activated in small numbers by specific antigens and expand clonally, this process takes 3 – 5 days to become evident. In the immunocompromised state of the body bacterial translocation takes effect, that is viable resident bacteria from gastrointestinal tract pass to sterile tissues[8]. This is facilitated by the destruction of mucosal barrier due to shock or pancreatitis in case of burn injuries. Expedited burn wound healing and management can help bypass many fatal complications.

2.2. Journey of skin substitutes/ scaffolds

Skin substitutes facilitate better healing in burns, and minimizes the risk of infections. It should be emphasized that these products are not active antimicrobial agents but rather serve as biocompatible barriers to prevent infection[9]. Nevertheless, they are frequently compared with the standard antimicrobial agent, silver sulfadiazine (AgSD). Their use results in a measured improvement in elasticity and flexibility of the healed burn, lessened scar contracture, reduction in the number of scar contracture procedures and plastic surgical reconstructions. The use of skin substitutes eliminates the need of changing dressings and repeated visits to the hospital clinics for that purpose.

The main disadvantage of cultured epidermal autografts and dermal substitutes is lack of consistency of performance mainly on wounds devoid of dermal elements[10,11] and insufficient donor sites[12] respectively. Hence, the requirement for a layer wise support was recognized. These substitutes are fragile in nature, require extreme care in patient's movement and require protection from infections to avoid loss of skin layers[13].

Biosynthetic skin substitutes (biological materials like collagen in combination with synthetic materials) include MatriDerm® (bovine collagen and an elastin hydrolysate) and Integra® Dermal Regeneration Template [a porous matrix of fibers of cross-linked bovine tendon collagen and glycosaminoglycan (chondroitin-6-sulfate)]. The most widely accepted artificial biological dermal substitute Integra®, faces serious complications against infections[14], though it is being countered by use of advanced antimicrobial silver dressings as overlay[15]. MatriDerm®, a newer generation artificial dermal substitute has an edge over Integra with faster degradation rate and promotion of vascularization via support of ingrowth cells and vessels[16].

Biological skin substitutes/Natural biological materials include decellularized human skin allografts like AlloDerm®, decellurized porcine xenografts like Permacol®, collagen derivatives, human amniotic membrane and cultured allografts. Though these provide better vascularization and adhesion, but are known for high cost, risk of transmission of infectious diseases and requirement for two surgical procedures[17].

Synthetic skin substitutes include Biobrane® (silicone film, nylon, collagen - derived peptides), Transcyte® (a porcine collagen-coated nylon mesh seeded with allogeneic neonatal human foreskin fibroblasts bonded to a silicon membrane), Dermagraft® (bioabsorbable polyglactin mesh scaffold seeded with cryopreserved allogeneic neonatal human foreskin fibroblasts), Actisorb® Silver 220 (Silver and activated charcoal dressing enclosed in a non-adherent nylon sleeve.), Allevyn® Gentle (soft gel adhesive) and Cutinova® Hydro (self-adhesive sterile wound dressing consisting of two layers - a polyurethane gel matrix and a polyurethane top-film). These products are currently in market but require further provisions for improvement and execution[16].

Dermal substitutes are generally costly. Biobrane® is the exact copy of Transcyte® without neonatal human fibroblasts. But Biobrane® is more famous with lower cost, easy to store and ease of application with reliable results[18]. There is high need to harness new technology that manage cost and navigate through regulatory norms.

A functional blend of natural and synthetic components is proposed as prospective answer for efficient management of second and third degree burn wounds economically.

3. Material and Methodology

3.1. Material and reagents used

Chemicals used in the fabrication and characterizations of the scaffold were procured from Sigma Aldrich (Delhi, India). All cell culture media and reagents were purchased from Thermo Scientific (Mumbai, India). Cell lines used in this study are from National Center of Cell Sciences (NCCS, Pune).

3.2. Fabrication of the scaffold

On semidried casted layer of hydrophobic polymer A, fibers of a mixture of polymer A and hydrophilic B containing antibiotics and bioactive agents were deposited. Subsequently, an aqueous solution of hydrophilic polymer C was poured and deep freezed.

3.3. Physicochemical characterization of scaffold

3.3.1. Scanning electron microscopy (SEM)

The morphologies of all layers and transverse sections of the scaffold were examined using the Field Emission Scanning Electron Microscope (FESEM Carl Zeiss Ultra Plus, Germany). The samples were initially fixed on stubs using carbon tape and gold coated at an accelerating voltage of 10-20 kV using a plasma gold sputter. Image J software was used to measure the fiber diameter of the samples taking 20 random fibres under consideration.

3.3.2. Mechanical properties

Uniaxial low load tensile tester (Bose Corporation Electroforce Systems Group, USA) was used to measure the tensile properties of BW scaffold, layer 1 and layer 2. The samples were sectioned into thin strips (5 mm width, 20 mm length and 2 mm gauge length). Vernier calipers (Fulcrum) were used to measure the thickness of the scaffold.

3.3.3. Contact angle

The hydrophilicity of all three layers of the scaffold individually was evaluated by the sessile drop technique. Water droplet of 2 μL was placed onto the scaffold surface and equilibrium angle between the scaffold surface and water droplet was determined.

3.3.4. Degradation kinetics

Trilayer BW scaffold samples were cut into strips (5 mm x 10 mm) and weighed to get the initial weight (W_i). Fluid medium closely resembling chemical and enzymatic profiles of burn wound exudate was used for this study and referred to as Simulated Burn Wound Exudate (SBWE)[19] (**Table 1**).

Table 1: Nominal ion concentration in SBWE formulation in comparison with those in blood plasma and burn wound exudate.

	Components	Blood plasma[20]	Burn exudate[21]	SBWE formulation[19]
1.	Na^+	142.0 mM	151.53 ±12.01 mM	142.0 mM
2.	K^+	5.0 mM	4.78 ±0.57 mM	5.0 mM
3.	Mg^{2+}	1.5 mM	0.90 ±0.16 mM	1.5 mM
4.	Ca^{2+}	2.5 mM	1.19 ±0.30 mM	2.5 mM
5.	Cl^-	103.0 mM	114.27 ±9.19 mM	147.8 mM
6.	HCO_3^-	27.0 mM	-	4.2 mM
7.	HPO_4^{2-}	1.0 mM	0.90 ±0.20 mM	1.0 mM
8.	SO_4^{2-}	0.5 mM	-	0.5 mM
9.	Urea	20 – 40 mg/dL	10.51 ±4.80 mM	10 mM
10.	Glucose	10 – 120 mg/dL	5.85 ±1.43 mM	6 mM
11.	pH	7.2 – 7.4	8.5 – 9.0	8.2

SBWE is made by procedure described by Kokubo and Takadama[19] with some modifications to mimic burn wound exudate. To make 1 L of SBWE, 700 mL deionized water was warmed up to 36.5 ±1.5°C while stirring. The constituents were dissolved one at a time in the order given in **Table 2** The temperature was maintained at 36.5 ±1.5°C as pH decreased with increasing temperature. Finally, the pH of the complete solution was adjusted to 8.2 and volume made up to 1 L. SBWE was stored at 4°C and used within 30 days.

Table 2: Order, amounts and formula weights of reagents for preparing 1000mL of SBWE mimicking burn wound exudate.

	Reagent	Amount
1.	NaCl	8.035 g
2.	$NaHCO_3$	0.355 g
3.	KCl	0.225 g
4.	$K_2HPO_4.3H_2O$	0.231 g
5.	$MgCl_2.6H_2O$	0.311 g
6.	$CaCl_2$	0.292 g
7.	Na_2SO_4	0.072 g
8.	Tris	6.118 g
9.	Urea	0.600 g
10.	Glucose	1.080 g
11.	0.1 M NaOH solution	To adjust pH

The SBWE was supplemented with enzymes, namely Matrix Metalloproteinase 2[22–24], Collagenase[25] and Lipase[26,27] according to their release profile observed in burn wounds (**Table 3**). The scaffold (5 mm x 10 mm) strips were incubated in 1 mL enzyme supplemented SBWE for 30 days at 37°C on a shaker with SBWE changes every second day. At specific time points, the samples were extracted and their wet (W_s) and dry weights (W_f) were recorded using microbalance.

Percent (%) degradation was calculated as: % Weight Loss = $((W_i - W_f)/ W_i) \times 100$

Table 3: Approximate enzyme release profile during burn injuries as observed in patients compiled from the literature.

Time points	Matrix Metalloproteinase 2[22–24] (ng/mL)	Collagenase[25] (ng/mL)	Lipase[26,27] (ng/mL)
0 h	200	70	550
6 h	200	300	550
12 h	200	200	550
18 h	225	150	550
24 h	225	100	550
36 h	250	120	550
48 h	275	120	550
3 day	300	190	550
4 day	400	150	550
5 day	450	160	550
7 day	500	170	550
13 day	300	150	550
23 day	300	90	550
30 day	100	50	550

3.3.5. Swelling behaviour

Trilayer BW scaffold swelling behaviour was observed along with the degradation for 30 days. The wet weight was recorded using microbalance at all time points and per cent (%) swelling for each time point was calculated as: $((W_s - W_f)/ W_f) \times 100$

3.3.6. Antibiotic and bioactive agent release study

The SBWE extracted at each time point in the degradation study contains the released antibiotics and bioactive agent present in the scaffold which were quantified through High-Pressure Liquid Chromatography (HPLC) (LC-2010 HT Liquid Chromatograph, Shimadzu, Japan) with a UV detector. C18 HPLC column (Ascentis C18, Supleco, Sigma) of 25 cm length, 4.6 mm inner diameter and 5 µm particle size was used. 70% acetonitrile was used to purge and store column after every use. Standards prepared in potassium phosphate buffer (0.2 M, pH 6.7) were run for calculating relative % release. Samples were first centrifuged at 3000 rpm for 10 minutes at 4°C, the supernatant filtered through 0.22 µm syringe filters and stored in HPLC vials at 4°C if not analysed immediately. The mobile phase used was 45% methanol and 55% potassium dihydrogen phosphate (5 mM, pH 6.3)[28].

3.3.7. Antimicrobial property

Antimicrobial property of antibiotic incorporated in the scaffold was confirmed on *Staphylococcus aureus* (isolated from Ganga, Rishikesh, procured from MTCC) and *E.coli* (DH5-Alpha Cells, procured from MTCC) by disc diffusion assay. Primary culture of *S.aureus* in nutrient broth (NB) and *E.coli* in Luria Bertani (LB) broth was set up for 12 hours. Secondary culture was set up at 0.1 optical density at 600 nm, incubated at 37°C bacteriological shaker incubator till the absorbance reached 0.4 – 0.5. 10 µL of the secondary culture and 90 µL of broth were mixed and spread on a NA agar plate for *S.aureus* and on LB agar plate for *E.coli*. Each plate was divided into following four quadrants:

1. Negative control: 5 µL drop of LB broth
2. Positive control: 5 µL drop of antibiotic (0.1 µg/µL concentration)
3. Control Scaffold: scaffold without antibiotic
4. Experimental Scaffold: scaffold with antibiotic

UV sterilized; 5 mm diameter scaffold discs were placed on respective quadrants on the plate. The plates were incubated at 37°C in a bacteriological incubator, and observed and imaged for the next 10 days for formation and maintenance of the zone of inhibition.

3.4.   *In-vitro* studies

3.4.1. Cell culture

For *in vitro* studies involving different layers of the scaffold, following cell lines were used:

- Layer 1 (outermost layer): HaCaT, an immortal keratinocyte cell line from adult human skin (National Centre For Cell Science (NCCS), Pune, India) cultured in DMEM high glucose media (passage no. 23-28).
- Layer 2 (middle layer): HDFa Primary Dermal Fibroblast; Normal, Human, Adult (National Centre For Cell Science (NCCS), Pune, India) cultured in DMEM High Glucose media (passage no. 25-31).
- Layer 3 (bottom-most layer): C3H/10T1/2, Clone 8, Mesenchymal Stem Cells (National Centre For Cell Science (NCCS), Pune, India) cultured in α-MEM media (passage no. 25-30).

The cells were maintained at 37°C tissue culture incubator with a steady supply of 5% CO_2, under 95% humidified conditions and subcultured when required.

3.4.2. Cell cytotoxicity assay

Scaffold layers were fabricated in various combinations to check their cytocompatibility by colourimetric MTT [3-(4,5-Dimethylthiazol-2-yl)-2,5-Diphenyltetrazolium Bromide] assay. The mitochondrial activity of live cells transforms yellow colored MTT to purple color formazon crystals. The design of the experiment included the following components/samples in triplicates:

1. Layer 1 Control: HaCaT (keratinocyte cell line) seeded directly on tissue culture plate

2. Layer 1 Scaffold: HaCaT (keratinocyte cell line) seeded onto scaffold

3. Layer 2 Control: HDF (dermal fibroblast cell line) seeded directly on tissue culture plate

4. Layer 2 Control Scaffold: HDF (dermal fibroblast cell line) seeded onto scaffold without antibiotics and bioactive agent.

5. Layer 2 Antibiotic Scaffold: HDF (dermal fibroblast cell line) seeded onto scaffold with antibiotics and without bioactive agent.

6. Layer 2 Bioactive Reagent Scaffold: HDF (dermal fibroblast cell line) seeded onto scaffold without antibiotics and with the bioactive agent.

7. Layer 2 Experimental/BW Scaffold: HDF (dermal fibroblast cell line) seeded onto scaffold with antibiotics and bioactive agent.

8. Layer 3 Control: C3H/10T1/2 (mesenchymal stem cells) seeded directly on tissue culture plate

9. Layer 3 Control Scaffold: C3H/10T1/2 (mesenchymal stem cells) seeded onto scaffold without a bioactive agent.

10. Layer 3 Experimental/BW Scaffold: C3H/10T1/2 (mesenchymal stem cells) seeded onto scaffold with the bioactive agent.

The scaffolds were cut, UV sterilized and placed in the wells of 96 well tissue culture plate. 5×10^3 fibroblasts, keratinocytes and mesenchymal stem cells were seeded per designated well and allowed to grow with regular replacement of culture medium every 24 hours. After 4 days, 10 µL of 5mg/mL MTT was added to each well and incubated for 4 hours at 37°C. Purple colored formazon crystals were dissolved in 100 µL DMSO (dimethyl sulfoxide) and absorbance recorded at 595 nm in a microplate reader (Biotek).

Percent cell viability was estimated as follows:

Cell Viability (%) = ((A_{595} Sample − A_{595} Control)/ A_{595} Control) x 100

3.4.3. Cell morphology and growth on the scaffold

The scaffolds were cut, UV sterilized and placed in the 96 well plate. The scaffolds were stained with Sudan black dye to curb the background fluorescence signal generated by the scaffold[29]. The scaffolds were incubated in their respective cell culture media overnight. 5×10^3 fibroblasts, keratinocytes and mesenchymal stem cells were seeded per designated well and allowed to grow for 4 days with regular replacement of culture medium every 24 hours. The cells were fixed for 15 minutes in a 4% formaldehyde at room temperature, washed with PBS and stained either with 4,6-diamidino-2-phenylindole (DAPI) or acridine orange/ethidium bromide (AO/EB) staining solution (1 μL) containing 100 μg/mL AO and 100 μg/mL EB (AO/EB). The samples were then mounted on slides and observed under an upright fluorescence microscope (Eclipse E100, Intensilight Epi-fluorescence Illuminator, Nikon) under appropriate filters.

3.4.4. SEM of cells on the scaffold

The scaffolds were cut, UV sterilized after placing in the 96 well plate and equilibrated in respective cell culture media overnight before seeding with designated cell lines. Cells were grown for 4 days. Layer 3 due to hydrogel composition retained moisture and hence was excluded from this experiment. The scaffolds were then washed with PBS, fixed in 4% formaldehyde and air-dried. The scaffolds containing cells were carefully fixed on the stubs and gold coated for 120 seconds at an accelerating voltage of 10-20 kV using a plasma gold sputter before examining under SEM.

3.4.5. Immunostaining of cells on the scaffold

Keratinocytes and fibroblasts were co-cultured on the respective sides of a scaffold containing layers 1 and 2 for 4 days in a snap well set up. The cells were washed with PBS, fixed with 4% formaldehyde, permeabilized with 0.1% TritonX-100, blocked in 5% BSA before incubating overnight with the primary antibody against tight junction protein *Zona occludens* (ZO-1) (Invitrogen, USA). FITC conjugated secondary antibody was used to fluorophore stain ZO-1. Phalloidin Alexa Fluor 555 was used to stain f-actin fibers. Cells

are counter stained with DAPI before imaging under confocal microscope (Nikon). Z-stacking was done to confirm the growth of keratinocytes and fibroblasts in different layers.

3.5.   *In-vivo* studies

3.5.1. Wound creation

Adult female Sprague-Dawley rats weighing 200 ± 50 g were used with approval from Institutional Animal Ethics Committee (IAEC) (approval no. MMCP-IAEC-10) following guidelines of Committee for the purpose of control and supervision of experimentation on animal (CPCSE, Govt. of India). Throughout the experimentation period, the animals were kept in a humidity and temperature-controlled room following 12 h photoperiod. The general health conditions of the animals were monitored and with access to food and water *ad libitum*. The animals were divided into following groups [n= 15 (3 animals at each time point x 5 time points) in each group].

Group 1: Untreated

Group 2: Standard burn ointment

Group 3: Standard scaffold for burn wounds

Group 4: Experimental scaffold

The animals were anaesthetized and dorsum shaved. A 100 g stainless steel rod (~1 cm in diameter) was heated in boiling water bath to 100°C and the rod rested on its own weight on flat surfaced skin which is firmly pulled upwards from the underlying viscera, for 5 seconds to create a 3rd degree burn wound[30,31]. UV sterilized scaffolds were soaked in autoclaved normal saline prior to application. According to the groups, the various treatments were given.

3.5.2. Wound closure studies

Wounds were photographed on day 3, 7, 12, 18 and 25 to evaluate the wound closure in each group. The wounds were physically measured and rate of wound closure calculated as:

% Wound closure = ((initial area of the wound - n^{th} day area of the wound) / initial area of the wound) x 100

3.5.3. Blood profiling

After 3, 7, 12, 18 and 25 days, blood was drawn through retro-orbital puncture for allergy and, liver and kidney toxicity tests that included Total Leukocyte Count (TLC), SGPT, SGOT, serum creatinine and serum urea assays.

3.5.4. HE staining of tissue samples

Portions of skin tissue from the injured areas were harvested after 3, 7, 12, 18 and 25 days, for histological studies through hematoxylin and eosin (H&E) staining. The tissues were fixed in Normal Buffered Saline (NBF) [100ml buffer containing 10ml 37% formaldehyde, 0.8g Sodium chloride (NaCl), 0.4g Dipotassium hydrogenphosphate (K_2HPO_4) and 0.65g Potassium dihydrogenphosphate (KH_2PO_4)] atleast overnight before dehydrating through alcohol gradation (30%, 50%, 70%, 90% and xylene). Dehydrated tissues were then embedded in molten paraffin wax to make blocks. Sections were cut out of these blocks using a microtome (Senior Rotary Microtome, Model: RMT-30, Radical Instruments). The sections were then stained with haematoxylin and eosin (HE). The sections were deparaffinised with xylene, rehydrated by dipping in a gradient of diluted ethanol (100%, 90%, 70%, 50%) for 2 minutes each, rinsed in tap water followed by staining in hematoxilin for 3 seconds. Excess hematoxylin washed out for 5minutes under running tap water and the sections were stained with eosin for 5 seconds. After a thorough wash with water, the sections were dried and mounted with coverslips in DPX Mountant. The stained sections were imaged under a light microscope (Carl Zeiss Axiovert, Germany).

4.   Results

4.1.   Characterization of the <u>B</u>urn <u>W</u>ound (BW) Scaffold

4.1.1.   Microscopic observations

The layer-wise structure of the tri-layer scaffold is illustrated in detail in **Figure 4A**. The layers were fabricated back-to-back along with their respective curing process. This measure increased the strength within each layer, maintained their topographical identity while facilitating adherence between layers.
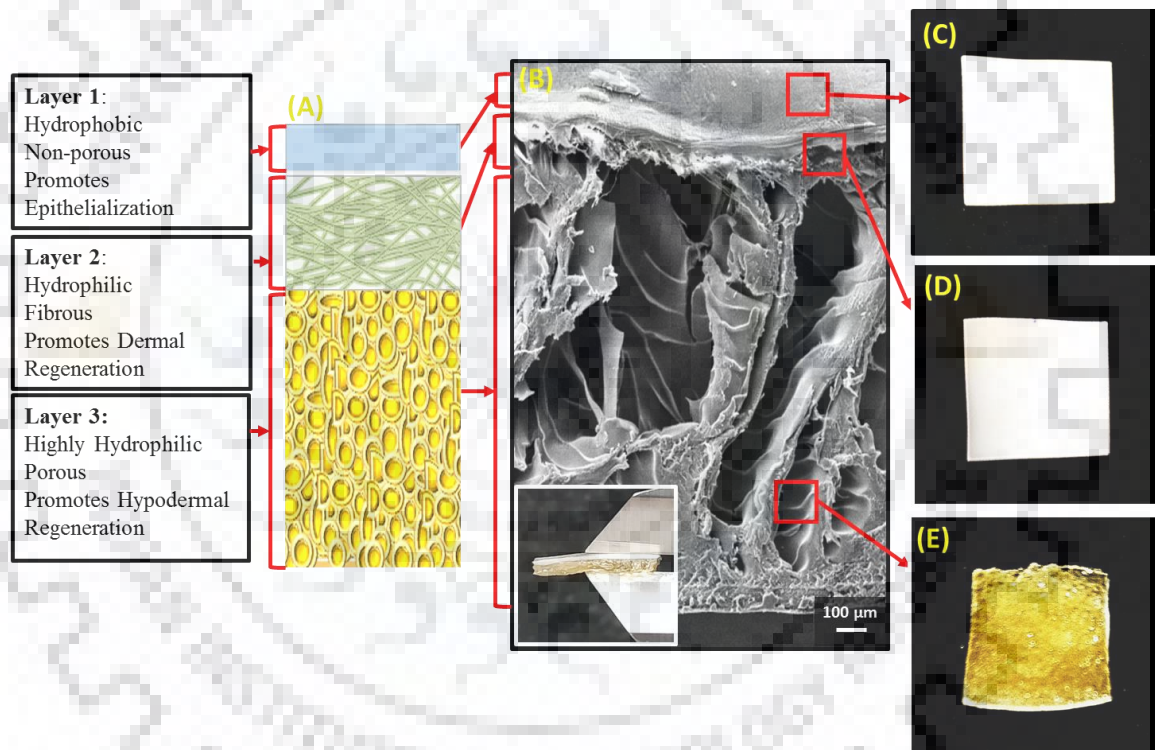

Figure 4: Appearance and microstructure of the BW Scaffold

[A] Schematic showing the structural architecture of the <u>B</u>urn <u>W</u>ound (BW) scaffold. **[B]** SEM image of the transverse section (TS) and each compositional zone of the scaffold (Inset: the optical image of a transverse section of BW Scaffold). **[C]** SEM image of Layer 1 non-porous surface topography (Inset: the optical image of Layer 1). **[D]** SEM image of Layer 2 porous surface topography (Inset: the optical image of Layer 2). **[E]** SEM image of Layer 3 highly porous surface topography (Inset: the optical image of Layer 3).

The transverse microstructure of the scaffold was imaged using Field Emission Scanning Electron Microscope (FESEM) (**Figure 4B**). An optical image of the transverse section of the scaffold is provided in the inset of **Figure 4B**. Field Emission Scanning Electron Microscope (FESEM) images of individual layers showing their surface topography are illustrated (**Figure 4C-4E**) and their optical images are provided in the inset of **Figures 4C-4E** respectively. The core-shell structure of the Layer 2 coaxially electrospun fibres was imaged by Transmission Electron Microscope (TEM) (**Figure 4F**).

The thickness of BW scaffold was found to be 1.34 ± 0.07 mm, where layer 1 is ~23.77 ± 1.69 µm, layer 2 ~69.69 ± 2.62 µm and layer 3 is ~1.14 ± 0.05 mm in width.

4.1.2. Contact Angle and Wettability of the scaffold

The engineered scaffold is also meant to facilitate the reconstructive phase of burn wound healing. This essentially requires specific architectural and moisture provisions in the form of varying ECM templates for simultaneous regeneration of all the layers of skin. Observations on the wettability of different layers of the scaffold and thus, their ability to provide for varying moisture requirements for the regeneration of different skin layers are provided in **Figure 5**.

The range of hydrophobicity across the scaffold due to compositional variations led to different wettability for different layers of the scaffold. By measuring the contact angles pertaining to different layers, the distribution of hydrophobicity across the depth of the scaffold was ascertained. Contact angles were measured using contact angle goniometer by the sessile drop method. Topmost layer 1 showed maximum hydrophobicity with a mean contact angle of 81.29 ± 0.68 (SE), followed by a mean contact angle of 60.34 ± 0.56 (SE) for middle layer 2. Mean contact angle reduces to 31.60 ± 0.77 (SE) for the bottom-most layer 3 (**Figure 5**& **Table 4**). With a decrease in the mean contact angles with each layer along the depth of the scaffold, the wettability increases: with maximum wettability designed to be in the vicinity of the hypodermis. This design is to efficiently support the simultaneous regeneration of all the layers of skin (each having a different moisture requirement) during the regenerative phase of burn wound healing.
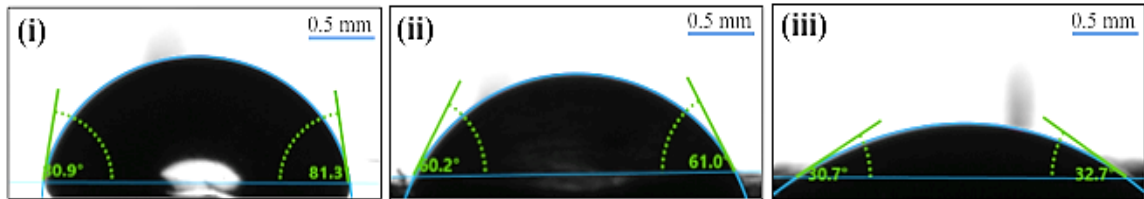
Figure 5: Wettability of the Scaffold

(i)-(iii) show the representative contact angle pictures pertaining to different layers within the BW scaffold. The corresponding mean values for each layer are also provided in **Table 5**.

Table 4: Table showing Mean Contact Angles of different layers with Standard Error (SE)

Panel Nos.	Layers of BW Scaffold	Mean Contact Angles ± SE
(i)	Layer 1	81.29 ± 0.68
(ii)	Layer 2	60.34 ± 0.56
(iii)	Layer 3	31.60 ± 0.77

4.1.3. Mechanical behaviour of the scaffold

The fabricated scaffold is not only meant for providing support for the regeneration of the layers of the skin but also to get remodelled into the skin tissue. Therefore, the mechanical properties of the scaffold, to begin with, should be in a similar range to that of natural skin. Thus, the mechanical behaviour of the fabricated scaffold was determined using a uniaxial tensile tester and the values were found to be well within the reported ranges for natural skin **(Figure 6 & Table 5)**.
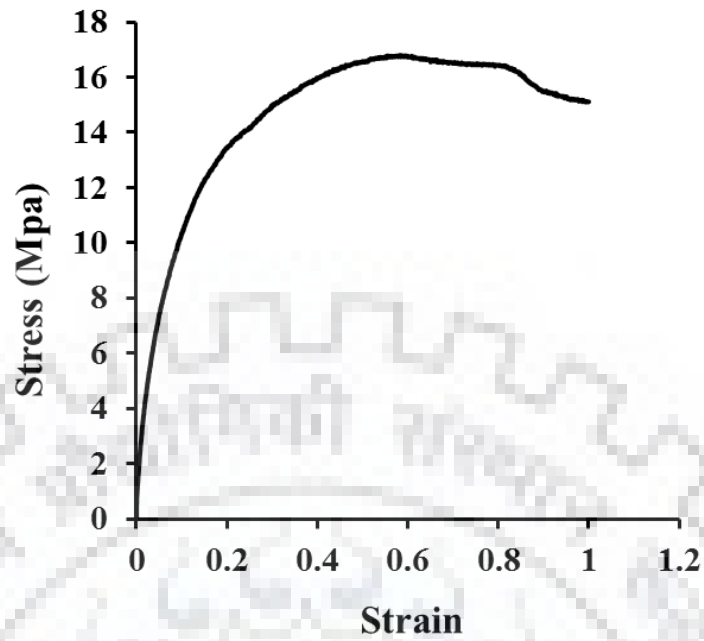
Figure 6: Mechanical Properties of the Scaffold

Stress versus strain curve of BW skin scaffold, cast layer 1, crosslinked and non-crosslinked layer 2.

Table 5: Showing Ultimate Tensile Strength and Young's Modulus*

Mechanical Properties	Burn Wound Scaffold	Human Skin
Ultimate Tensile Strength (UTS) (MPa)	16.79 ± 0.77	27.2 ± 9.3[32]
Young's Modulus (E) (MPa)	102.22 ± 2.43	0.005 − 140[33]

* Data is represented as mean ± standard error (SE) of values obtained from three independent experiments.

4.1.4. In vitro dissolution of the scaffold

Coping with the secreted exudate, bacterial infection, acute inflammation and scar-free reconstruction of the damaged tissue are the challenges associated with burn wound management. The composition of the trilayer scaffold is entirely biodegradable and is engineered to facilitate exudate management, provide protection against bacterial infection, soothe inflammation and eventually get remodeled into the skin tissue. To ensure the efficacy of the scaffold in addressing these issues *in vivo*, these properties were evaluated *in vitro* through dissolution, swelling and antibiotic and anti-inflammatory/regenerative agent release profiling. *In vivo*, the scaffolds are exposed to burn wound exudate after implantation. Therefore, the profiling study was conducted in a medium with composition closely resembling that of burn wound exudate and referred to as Simulated Burn Wound Exudate (SBWE). The designing of simulated burn wound exudate not only mimics the chemical profile but also the enzyme profile of the burn wound exudate, to the point of following the subsequent changes seen in the enzyme profile during the course of 30 days (**Figure 7**). Matrix metalloproteinase 2 (MMP2), collagenase and lipase are the main enzymes present in burn wound exudate, which will play a crucial role in the degradation of the scaffold.

The loss in weight of the scaffold at particular time intervals was measured to follow the rate of dissolution. The dissolution rate of the whole scaffold was found to be very fast (**Figure 7**) due to the composition of layer 3. Almost 80% of the scaffold (mainly comprising of Layer 3) dissolved within the first two days of incubation. In the context of *in vivo* healing of the wound in the rat model, this observation falls in line as the scaffold treated group of animals indeed exhibited visibly expedited puss-free healing during the first three days of treatment. This implicates that the scaffold is effectively getting bioresorbed into the system and getting remodeled as skin tissue thereby, speeding up the healing process. The remaining 20%, comprising of layers 1 and 2, showing unrushed dissolution will be instrumental in keeping out infection and facilitating tissue remodeling in the reconstructive phase of healing.
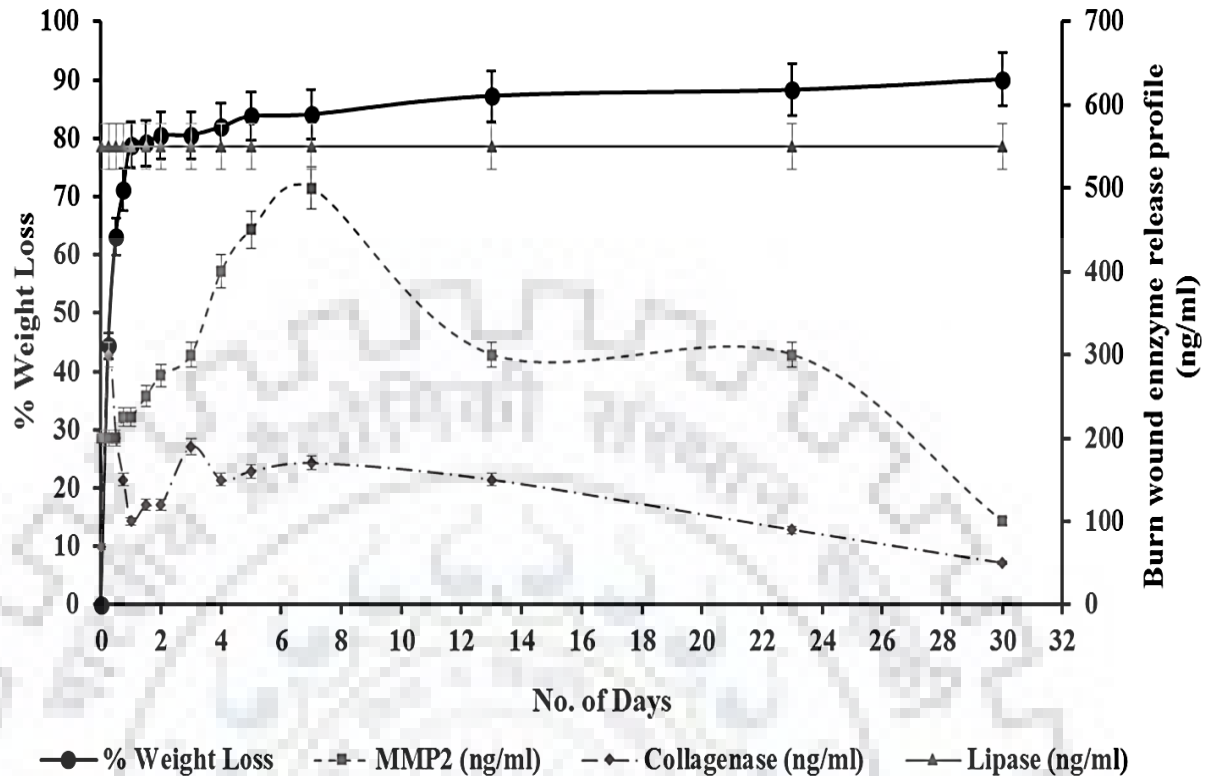
Figure 7: Graph showing per cent (%) weight loss of the scaffold with all the three layers along with the observed enzyme release profiles over a period of thirty days. Scaffold incubation was done in **S**imulated **B**urn **W**ound **E**xudate (**SBWE**). Each data point represents the a*vera*ge % weight loss/release ± standard error (SE). Samples were evaluated in triplicates for each time point.

4.1.5. In vitro exudate management by swelling assay

Burn wound exudate contains factors, which can be both facilitative and detrimental for healing. It contains pro-neovasculogenic, pro-inflammatory and fibroblast proliferative agents. If not sequestered spatially to the zone requiring it the most, burn wound exudate might prove to be inimical to the healing process. Being pro-proliferative for fibroblasts, improper management of exudate can lead to pervasive fibroblastic growth, eventually leading to scarring and imperiling tissue reconstruction. In addition, being rich in growth factors, exudate, if not sequestered and managed, leads to bacterial infection. Thus, for proper healing of full-thickness burn wounds, exudate scavenging and

sequestration are critical. The third layer has been designed specifically for this purpose. Therefore, the trilayer scaffold was tested for its ability to absorb exudate through swelling assay.
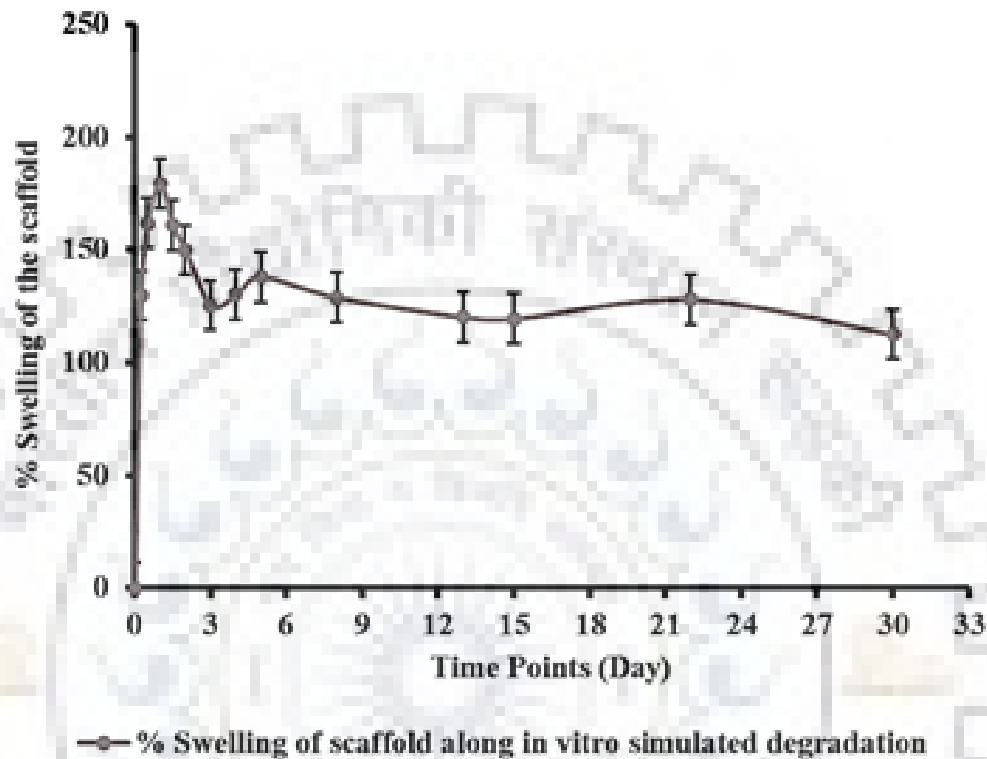

Figure 8: Graph showing per cent (%) swelling of the complete scaffold over thirty days. Scaffold incubation was done in **S**imulated **B**urn **W**ound **E**xudate (**SBWE**). Each data point represents the *avera*ge % weight loss/release ± standard error (SE). Samples were evaluated in triplicates for each time point.

The observations showed almost 130% swelling of the scaffold within 24 hours of incubation. This value increased to 180% by one and a half day. Thereafter, it dropped to 130% and remained more or less constant until 30 days. The extensive swelling within a few hours of incubation can be attributed to the hygroscopic nature of layer 3. *In vivo*, this will facilitate efficient exudate absorption immediately after scaffold implantation. The dip and subsequent consistency in per cent swelling are due to the dissolution of layer 3 with concomitant exposure of comparatively less hydrophilic layer 2. While *in vitro*, the layer

3 dissolves into the SBWE, *in vivo* scenario will be slightly different. The layer 3 will not dissolve away readily, rather it will swell with burn wound exudate and become an active ECM for cell proliferation (**Figure 8**).

4.1.6. Antibiotic and anti-inflammatory agent release profiling

The simulated burn wound exudate was collected at fixed intervals of scaffold incubation and analyzed for the presence of antibiotic A and bioactive components through high performance liquid chromatography (HPLC)[28], and presence of antibiotic B through colorimetric indirect UV assay as it low absorbance on UV Vis spectra[34]. 90% and 74.5% cumulative release of antibiotic A (**Figure 9A**) and antibiotic B (**Figure 10A**), respectively, was observed by third-day post incubation (resembling third-day post-injury *in vivo*). Thereafter, the release drops. Burn wounds are at the highest risk of bacterial infection between 48-72 hours of burn injury when the inherent defence of the body gets exhausted.

So, the observed antibiotic release profile showing maximum release around this time will be in congruence with expected reinforcement against anticipated ensuing bacterial infection *in vivo*. The released antibiotics were stable even after 10 days (as shown through disc diffusion assay in **Figure 13**). In addition, the antibiotics are likely to remain in the neighborhood of the damaged tissue for longer due to exudate sequestration. Hence, bacterial infections will be taken care of even beyond 72 hours. The bioactive components are released 11% within 6 hours of the scaffold coming in contact with the simulated exudate. This release starts dropping from the third day of incubation where 70% anti-inflammatory agent has been released and the rest 30% exhausts by the fifteenth day (**Figure 11**). This provides an initial soothing effect to the wound and later on helps to keep inflammation at bay. In addition, being pro-neovasculogenic, continuous late release (time coinciding with a reparative phase of *in vivo* scenario) of this agent will facilitate blood vessel formation.
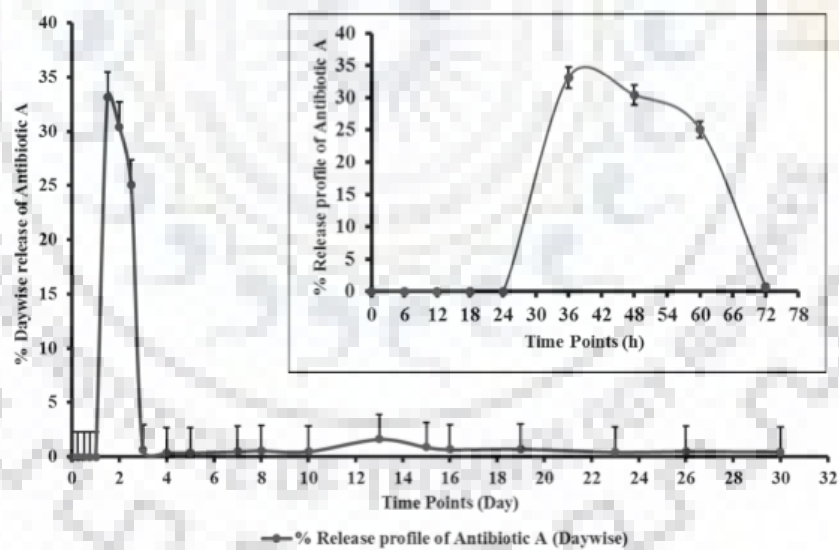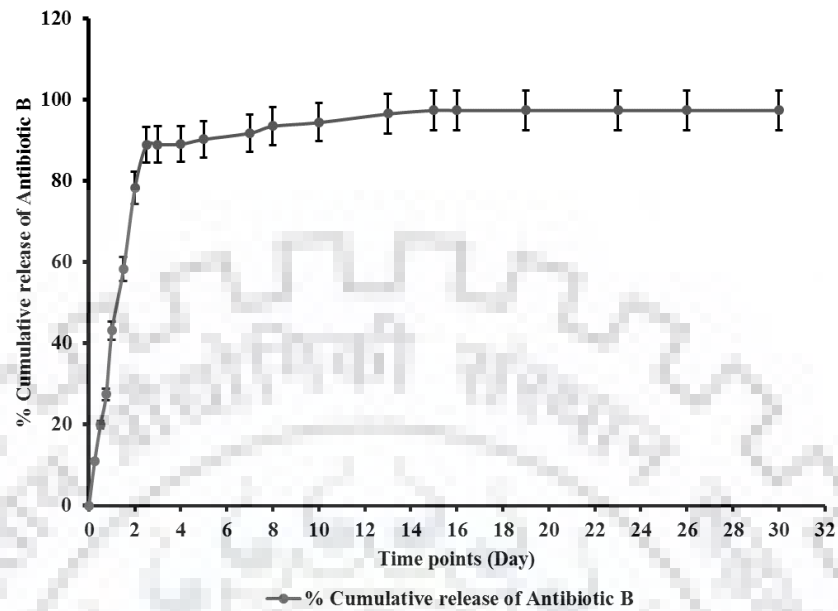
[A]
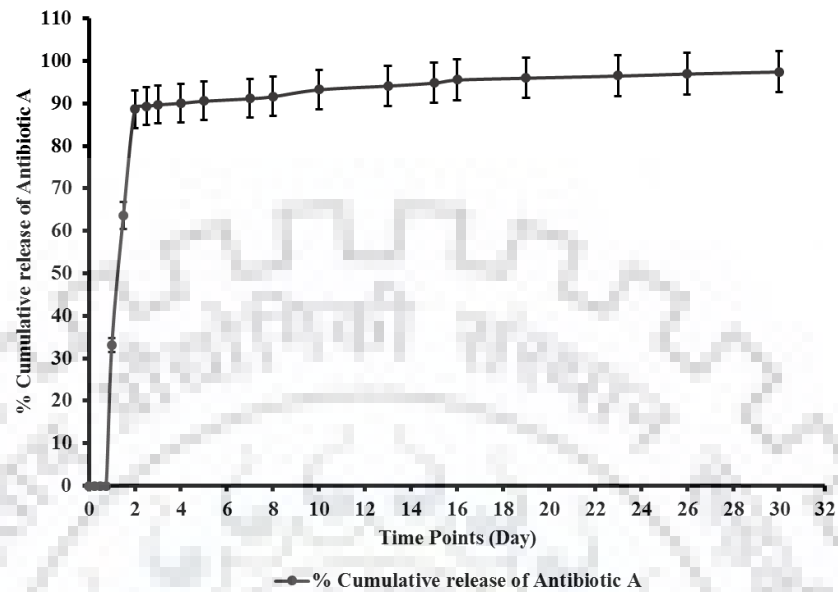
[B]

Figure 9: Graph showing the percent (%) cumulative [A] and day wise [B] (B Inset: release profile of vancomycin for the initial 72 hours) release of antibiotic antibiotic A. Scaffold incubation was done in **S**imulated **B**urn **W**ound **E**xudate **(SBWE)**. Each data point represents the a*vera*ge % weight loss/release ± standard error (SE). Samples were evaluated in triplicates for each time point.
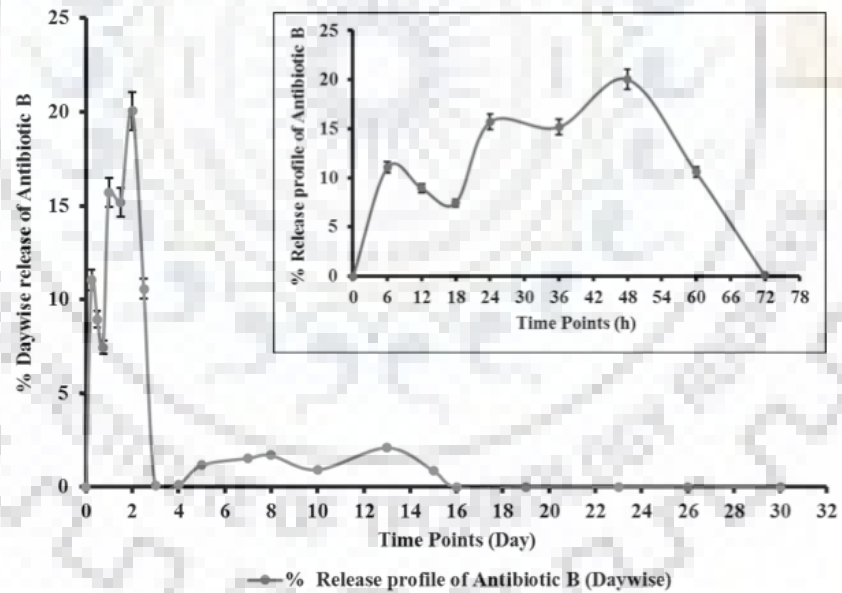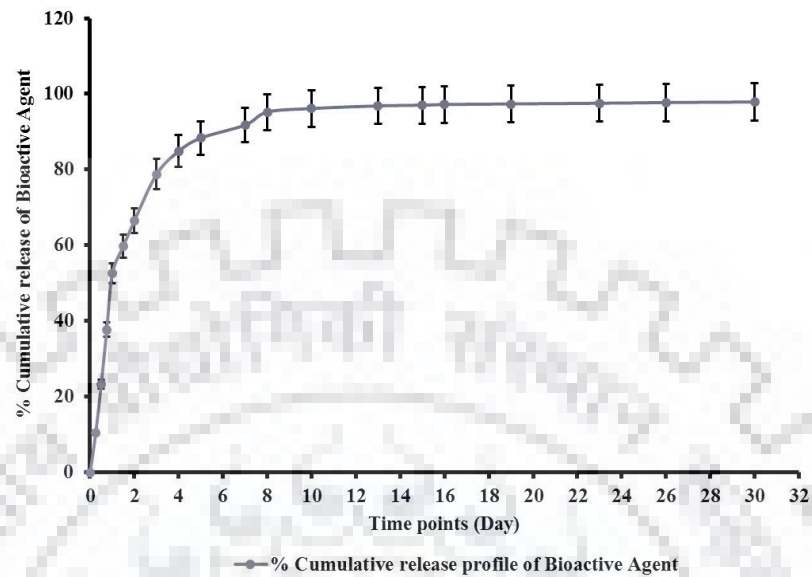
[A]

[B]

Figure 10: Graph showing the percent (%) cumulative [A] and day wise [B] (B Inset: release profile of gentamicin for the initial 72 hours) release of antibiotic antibiotic B. Scaffold incubation was done in **S**imulated **B**urn **W**ound **E**xudate **(SBWE)**. Each data point represents the a*vera*ge % weight loss/release ± standard error (SE). Samples were evaluated in triplicates for each time point.
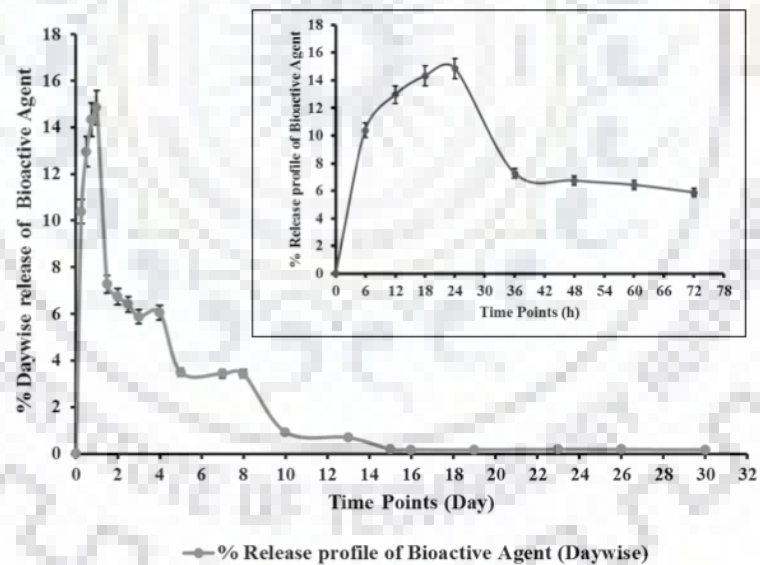
[A]

[B]

Figure 11: Graph showing the per cent (%) cumulative [A] and day wise [B] (B Inset: release profile of bioactive agent for the initial 72 hours) release of *bioactive agent*. Scaffold incubation was done in **S**imulated **B**urn **W**ound **E**xudate **(SBWE)**. Each data point represents the a*vera*ge % weight loss/release ± standard error (SE). Samples were evaluated in triplicates for each time point.

[A]

[B]

Figure 12: Graph showing the per cent (%) cumulative [A] and day wise [B] (B Inset: release profile of acemannan for the initial 72 hours) release of *anti-inflammatory component*. Scaffold incubation was done in **S**imulated **B**urn **W**ound **E**xudate **(SBWE)**. Each data point represents the a*vera*ge % weight loss/release ± standard error (SE). Samples were evaluated in triplicates for each time point.
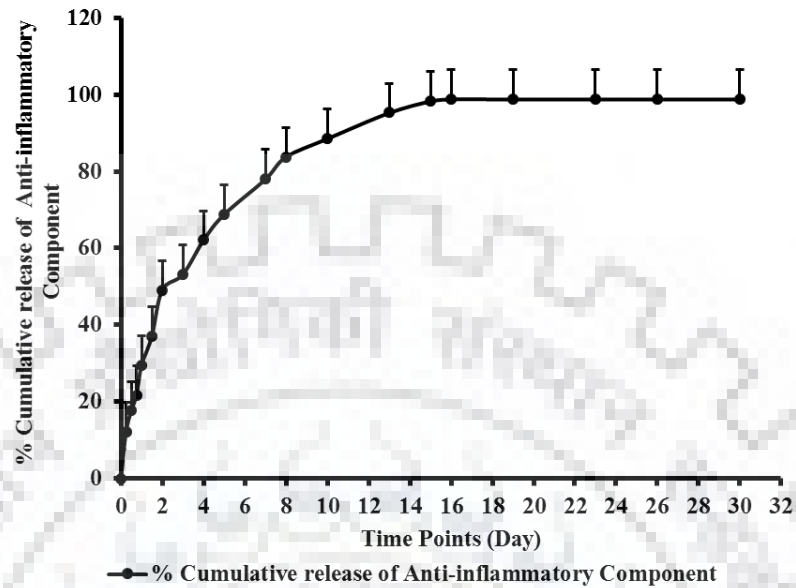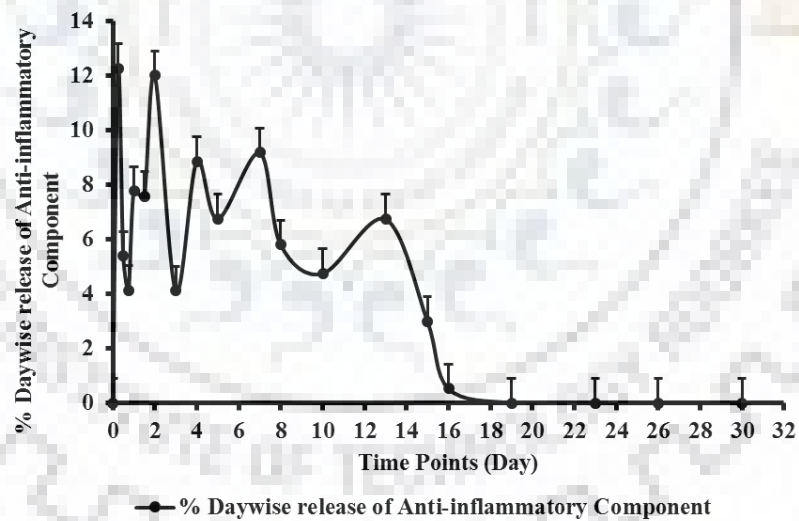
The bioactive agent used in the BW scaffold is known mainly for its immunostimulant, pro-proliferative, anti-inflammatory and anti-viral properties among others. The presence and release of anti-inflammatory component in the SBWE was confirmed by colorimetric assay, where Congo Red dye is used as the indicator compound. 60% cumulative release of the anti-inflammatory agent was observed by day 4 and attains maximum release by day 16 (**Figure 12**). There is a constant release of this agent for 16 days and its constant presence in burn wound bed will expedite the healing process.

4.1.7. Antibacterial disc diffusion assay

The strength and gradual release of the vancomycin and gentamicin from the experimental scaffold were confirmed by antibacterial disc diffusion assay (**Figure 15**) on gram-negative *E.coli* (**Figure 15A**) and gram-positive *S.aureus* (**Figure 15B**) bacteria.
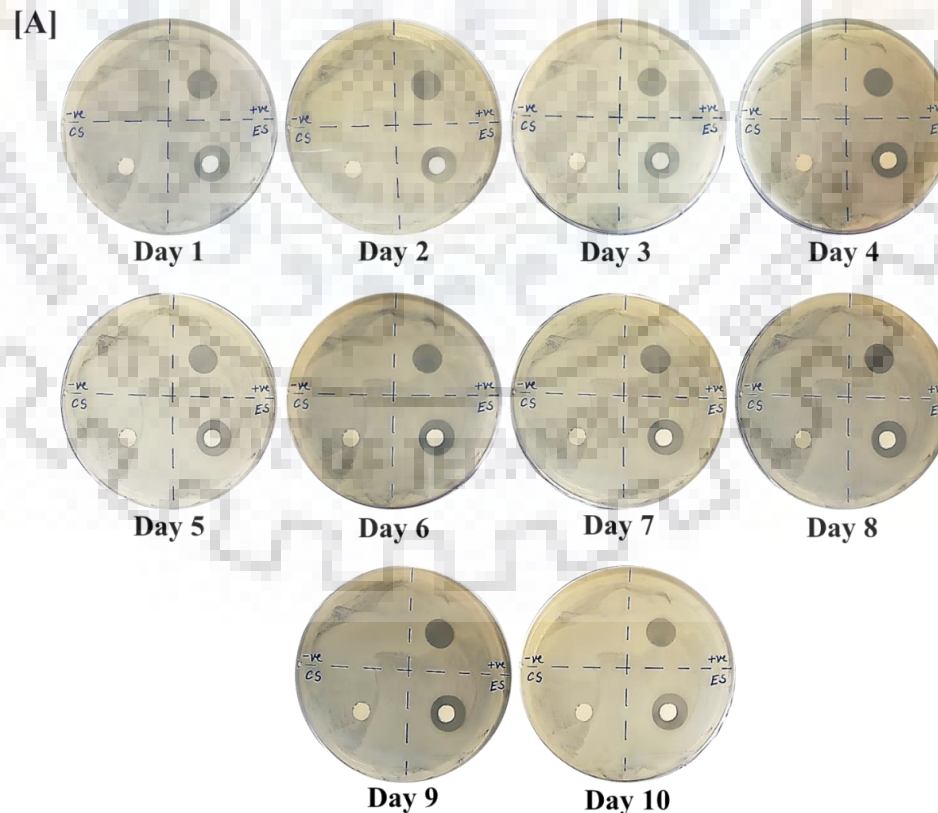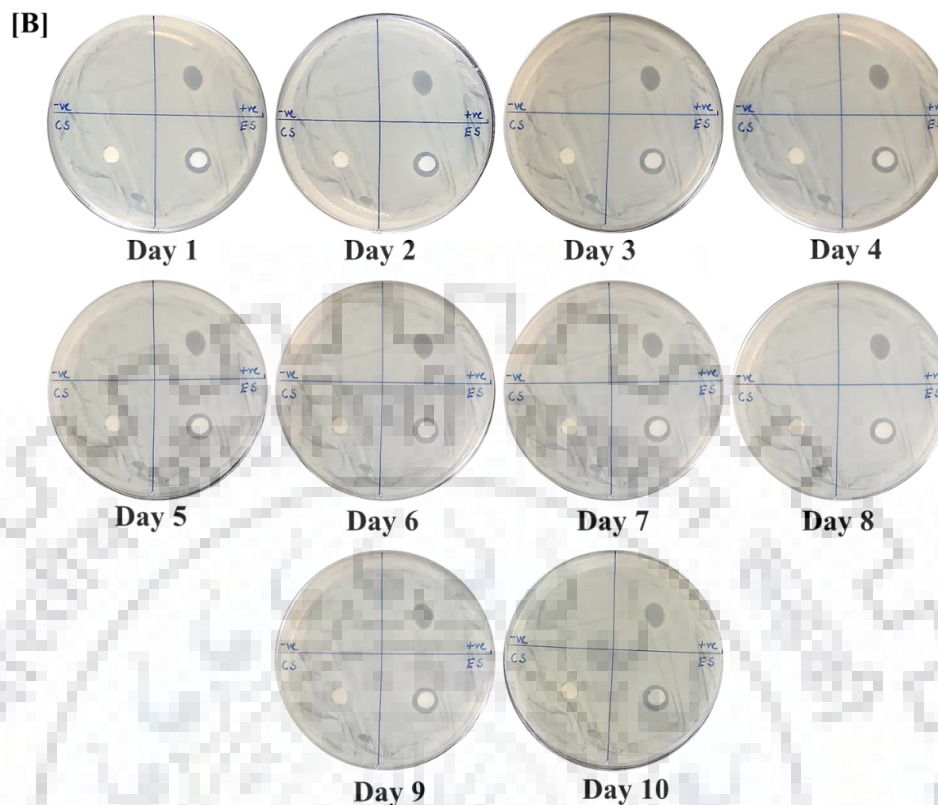
Figure 13: Antibiotic release study by the formation of zone of inhibition on bacterial lawn. Continuous diffusion and effectiveness of the antibiotics incorporated in the scaffold established by disc diffusion assay. **[A]** *E.coli* and **[B]** *S.aureus*.

The agar plates with bacterial lawn on them were divided into four quadrants. No antibiotic (-ve), antibiotics at a similar concentration as present in the experimental scaffold (ES) (+ve) and control scaffold without antibiotics (CS) were included as negative, positive and experimental controls. The plates were monitored and imaged for 10 days. Quadrant with positive (+ve) control showed a clear zone of inhibition right after 24 hours (Day 1) of incubation. Control scaffold (CS) did not form any zone of inhibition even after 10 days. Experimental scaffold (ES), like, positive control formed and maintained a clear zone of inhibition, impenetrable by the bacteria, over 10 days.

4.2.   Evaluation of biocompatibility of the BW scaffold

Natural skin is composed of keratinocytes (epidermis) and fibroblasts (dermis). Therefore, cytocompatibility of the burn wound-healing scaffold was checked for both the types of cells by monitoring their viability through MTT assay. In addition cytotoxic effects were also evaluated on mesenchymal stem cells (MSCs) because regeneration of hypodermis and underlying skeletal muscles will involve MSCs. The layers 1, 2 and 3 of the experimental scaffold were independently seeded with HaCaT (keratinocytes, NCCS), PCS-201 (human dermal fibroblast, HDFa, NCCS) and Murine C3H10T1/2 (mesenchymal stem cells (MSCs), NCCS) cells, respectively and cytotoxicity assayed after 4 days of incubation. Each of these cells pertained to the type of cells that constitute the corresponding layer of the skin. Same cells grown on tissue culture dish were taken as control. A control scaffold without antibiotics and/or bioactive agent/ or without only bioactive agent was included incase of layer 2 and layer 3, respectively was included to rule out any deleterious effect on cell growth due to the presence of antibiotic and bioactive agent alone or in combination. Actively growing cells convert MTT to formazan crystals. DMSO can dissolve these crystals to produce a purple solution. The intensity of purple color and thus, the corresponding optical density at 570nm (OD_{570}) are directly proportional to the number of surviving cells and represented as percent survival relative to the control. The experimental scaffold supported nearly 40% more fibroblast and 45% more mesenchymal stem cell growth relative to respective controls. Corresponding control scaffolds showed cell survival similar to that of experimental scaffolds. Similar keratinocyte survival was observed for scaffold and its corresponding tissue culture dish control (**Figure 14**). This indicated that the scaffold material was not toxic to the cells and that it provided a substratum better than tissue culture dish. This data also confirmed that the degradation products released from the scaffold were non-toxic and hence, did not jeopardize metabolic activities of the cells growing on them.
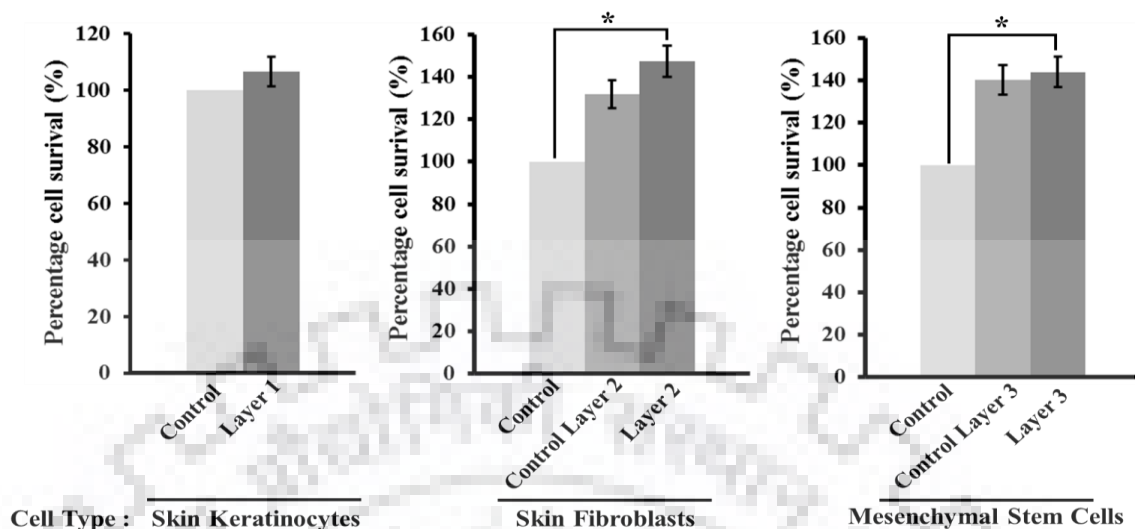
Figure 14: Histogram showing percent (%) survival of keratinocytes, fibroblasts and mesenchymal stem cells after 4 days of incubation on BW skin scaffold evaluated by MTT assay. Each data point represents mean ± standard error (SE) of values from three independent experiments (* p value < 0.05).

In addition, nuclei of the keratinocytes and dermal fibroblasts grown individually on the scaffold in an array similar to that used for MTT assay were stained with DAPI to observe the nuclear integrity. Like earlier, respective cell lines grown on tissue culture plates were included as controls. Confirming the MTT data, nuclear staining showed higher population density of keratinocytes, fibroblasts and mesenchymal stem cells when grown for identical durations on scaffolds as compared to tissue culture plates **(Figure 15)**. The nuclei also showed intact chromatin (seen as bluish threads in the magnified images of the nuclei provided in the insets) and un-fragmented nucleoli (indicated with white arrows in the insets). This shows that the scaffold has no apparent deleterious effect, like, chromosomal or nucleolar fragmentation on the cells, ruling out any associated genotoxicity. This observation was corroborated by Acridine-Orange/ Ethidium Bromide (AO-EB) staining of the cells **(Figure 16)**, in addition to confirming absence of apoptosis and/or necrosis. Surface morphology of keratinocytes and dermal fibroblasts and enhanced growth of fibroblasts on BW scaffold were evaluated through SEM images **(Figure 17)**.

In order to evaluate the effect of the scaffold fortification on paracrine activities of different types of skin cells, keratinocytes and dermal fibroblasts were co-cultured for 4 days on the layer 1 and layer 2 of the scaffold and immunostained for specific markers: *zona occludens* (ZO-1) for keratinocytes and *f-actin* for fibroblasts. Scaffold lacking antibiotic and bioactive fortification (Control Scaffold) was included as experimental standard for the traits being evaluated. Compared to cover slip, growth of both keratinocytes and dermal fibroblasts was found to be enhanced when co-cultured on the scaffold Expression levels of ZO-1 and *f-actin* and their correct sub-cellular distribution in the cells grown on scaffolds (as compared to control; cells were grown on cover slip) confirmed healthy cellular physiology.
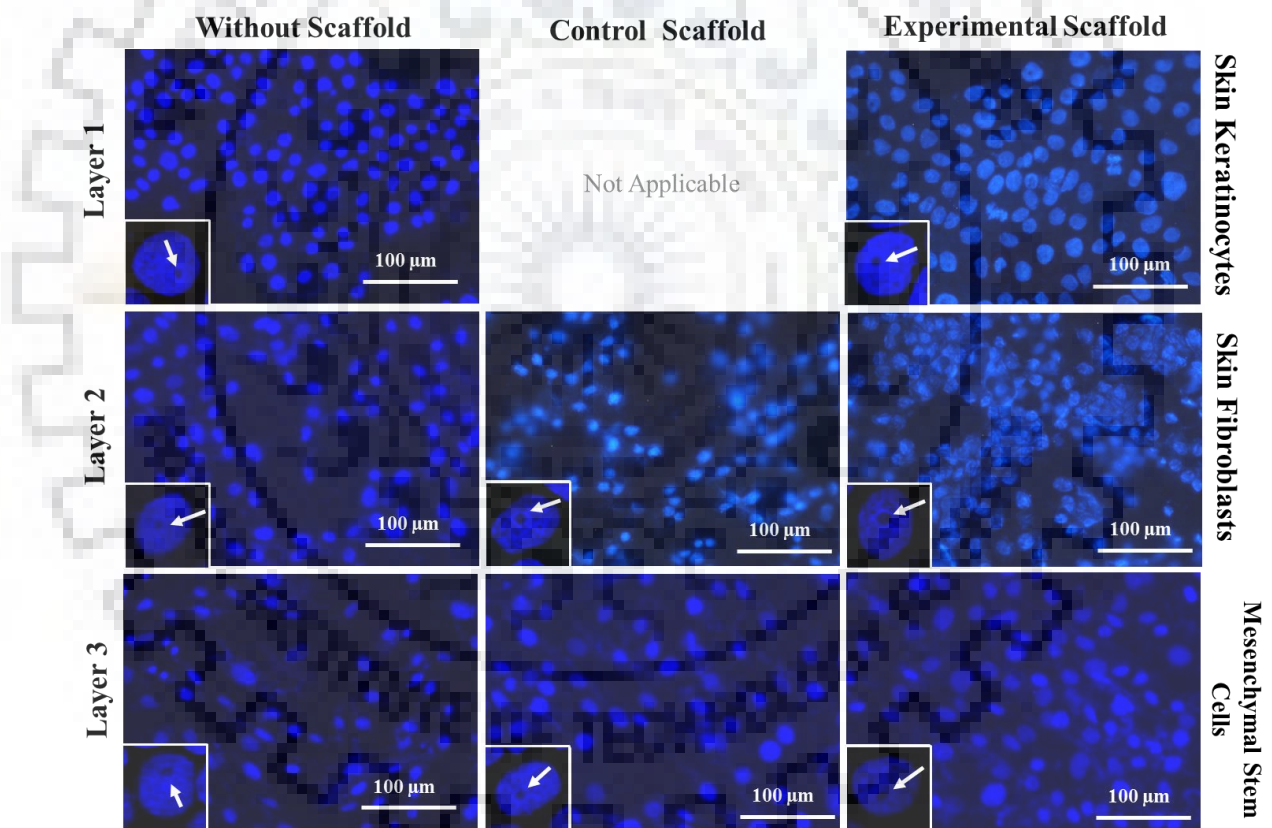

Figure 15: Enhanced growth and absence of genotoxicity in keratinocytes, fibroblasts and mesenchymal stem cells cultured individually, on corresponding suitable layers of the scaffold are shown through representative DAPI staining. Magnified view of representative DAPI stained nuclei (insets) showing intact chromatin and un-fragmented nucleoli (indicated by white arrows).
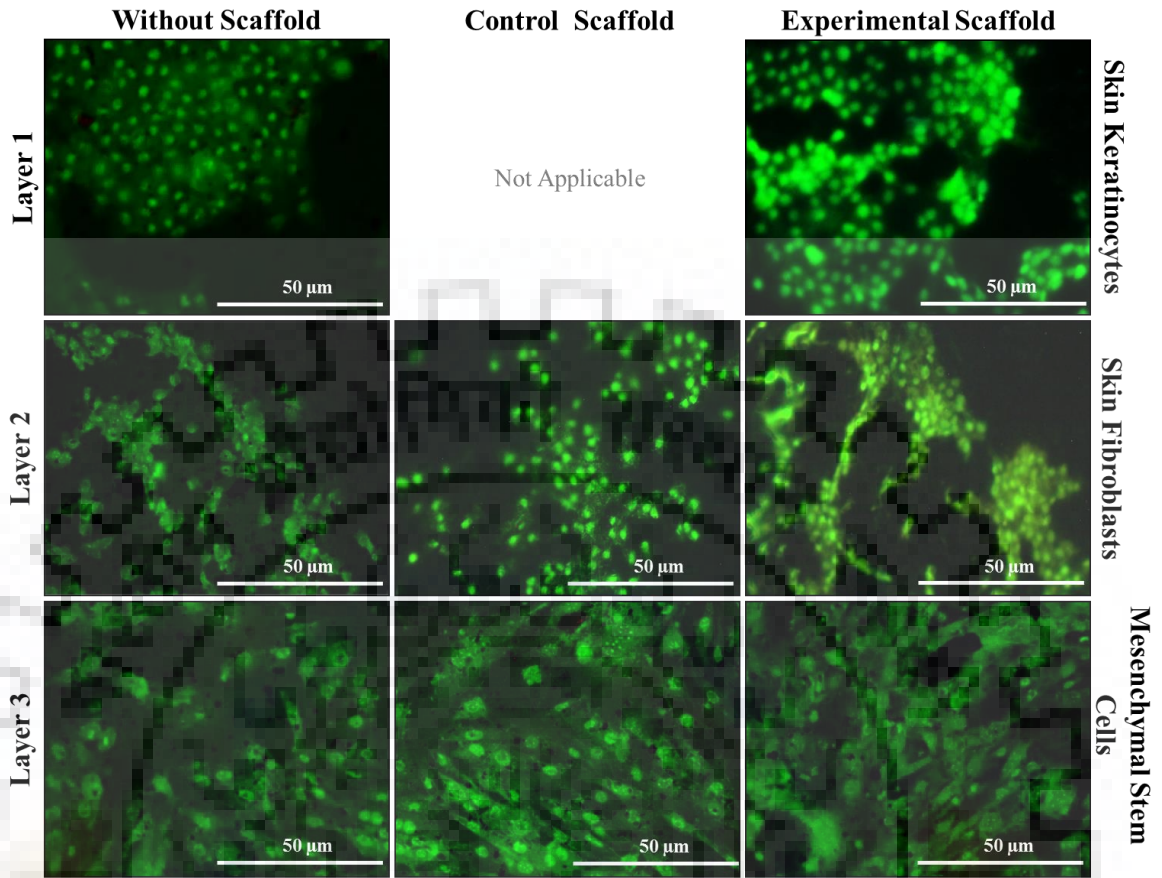
Without Scaffold **Control Scaffold** **Experimental Scaffold**

Layer 1

Layer 2

Layer 3

Skin Keratinocytes

Skin Fibroblasts

Mesenchymal Stem Cells

Not Applicable

50 μm

50 μm

50 μm

50 μm

50 μm

50 μm

50 μm

Figure 16: Enhanced growth and absence of apoptosis and/or necrosis in keratinocytes, fibroblasts and mesenchymal stem cells cultured individually, on corresponding suitable layers of the scaffold are shown through representative Acridine-Orange/ Ethidium Bromide (AO-EB) staining.

Layer 1

Layer 2

Control Scaffold **Experimental Scaffold**

20 μm

20 μm

20 μm
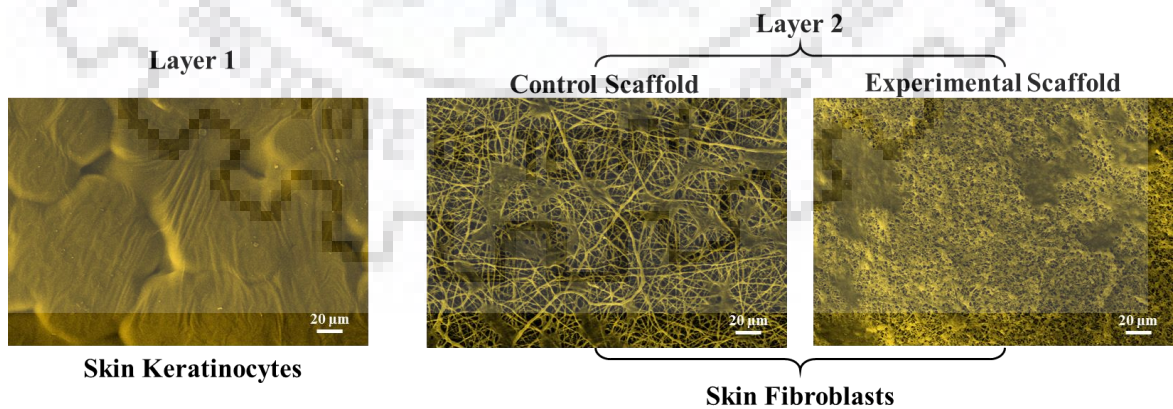
Skin Keratinocytes

Skin Fibroblasts

Figure 17: Morphologies of the cultured keratinocytes and fibroblasts cells on scaffold are shown through SEM images. Layer 2 with different compositions is compared.

Enhanced membrane localization of ZO-1 and prominent fibrillar appearance of *f-actin* in case of cells co-cultures on experimental scaffold compared to control scaffold, shows improved inter-cellular cross-talks and improved paracrine activities **(Figure 18)**. This implicates that fortification of the scaffold with antibiotics and bioactive agent is salubrious for simultaneous growth and proliferation of different populations of cell. *In vivo*, this will translate into improved tissue organization during healing. The capability of the experimental scaffold in preventing random mixing of different cell populations, particularly, restricting the highly proliferative dermal fibroblasts to the middle layer and preventing them from invading the top layer was confirmed **(Figure 19)**.

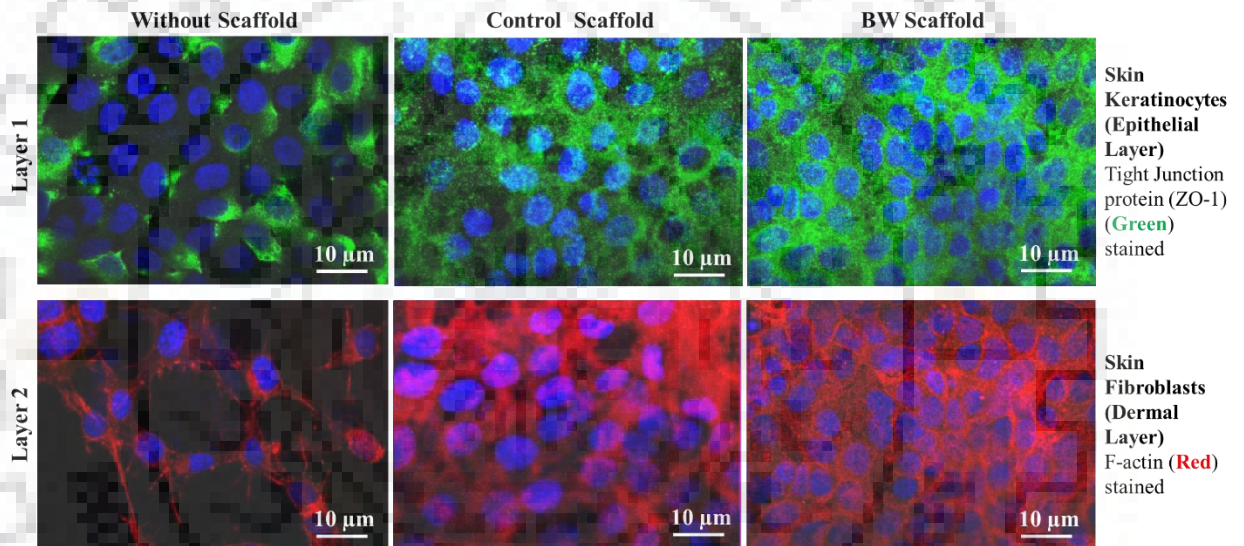**Figure 18:** Healthy coexistence and improved physiology of keratinocytes and fibroblasts co-cultured for 4 days on specific layers of the scaffold is shown through representative immunostaining of Zona Occludens (ZO-1) (green) and *f-actin* (red) respectively.
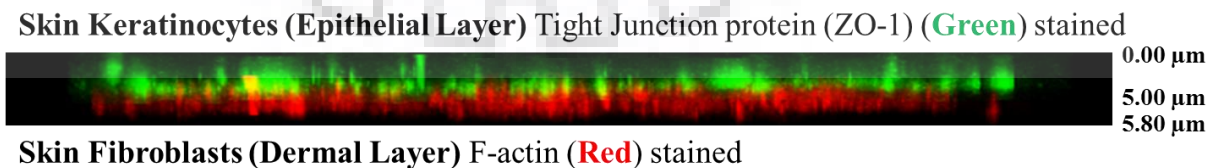

Figure 19: BW scaffold maintained dermal fibroblasts and keratinocytes in their designated regions as evident from z-stacking.

4.3. Evaluation of the efficacy of the designed scaffold in healing skin wound *in vivo*

The efficiency of the scaffold in healing full thickness burn wounds was evaluated *in vivo* on burn wound model of Sprague Dawley (SD) rats. The animals were divided into four groups: untreated (with untreated wounds), Standard [where the wound was treated with standard burn ointment (containing 0.2% by wt. silver compound)], Standard Scaffold (where wound was treated with Aquacel Ag$^+$ Extra from ConvaTec, a commercially available scaffold for burn wound healing) and Experimental Scaffold (where wound was treated with a scaffold fortified with antibiotic or bioactive agent). 10 mm burn wounds were inflicted with solid 100 g stainless-steel rods heated to 100°C. The digital images of the gross appearance of wounds for all categories are shown in **Figure 20** for different post-injury time intervals. The rate of wound closure/ reduction in wound diameter was used as an indicator for healing efficiency of the scaffold**.** The animals were observed for 25 days, during which optical images and reduction in dimensions of the healing wounds were recorded. After 25 days of wound infliction, around 45% of the wound was closed in the animals belonging to the untreated group (Positive group). Around 53.3% and 61.6% wound closure was observed in case of the animals treated with Burn ointment (Standard group) and commercially available scaffold (Standard Scaffold group), respectively. This percentage increased to 98.5% for the animals treated with the experimental scaffold (Scaffold group) by 18th day and 100% by 25th day **(Figure 20)**.

During early time points of healing, the ground is set up for expedited healing in animals belonging to Experimental Scaffold group. This includes scavenging and sequestration of exudate, wound soothening, prevention of aggravation of inflammation and protection against bacterial infection. The experimental scaffold is in the process of integrating with the body. This argument appears more logical when a sudden improvement in wound closure in the Experimental Scaffold group is seen 7th day onwards till almost 99% of the wound gets closed by 18th day. The wound closure kinetics for standard scaffold is slightly faster than standard ointment and being left untreated. However, almost similar slope of the graphs pertaining to standard scaffold, standard and untreated groups indicates that the commercially available scaffold does not modulate the natural healing process *per*

se, except may be for providing protection from bacterial infection. The slightly better kinetics, that is visible for standard and standard scaffold groups when compared to the untreated group, is likely due to the initial boost received in the form of protection from bacterial infection and prevention of spreading of wound bed. Wound closure kinetics of the Standard Scaffold group improved slightly 12th day onwards. By 12th day, the body starts replacing damaged tissue with its repertoire of stem cells. Being collagen based, the standard scaffold is likely to provide the extracellular matrix (ECM) for faster proliferation of cells. Eventually, this manifests as improved wound closure by 18th and 25th days. However, the experimental scaffold still outstands in wound closure **(Figure 21).**
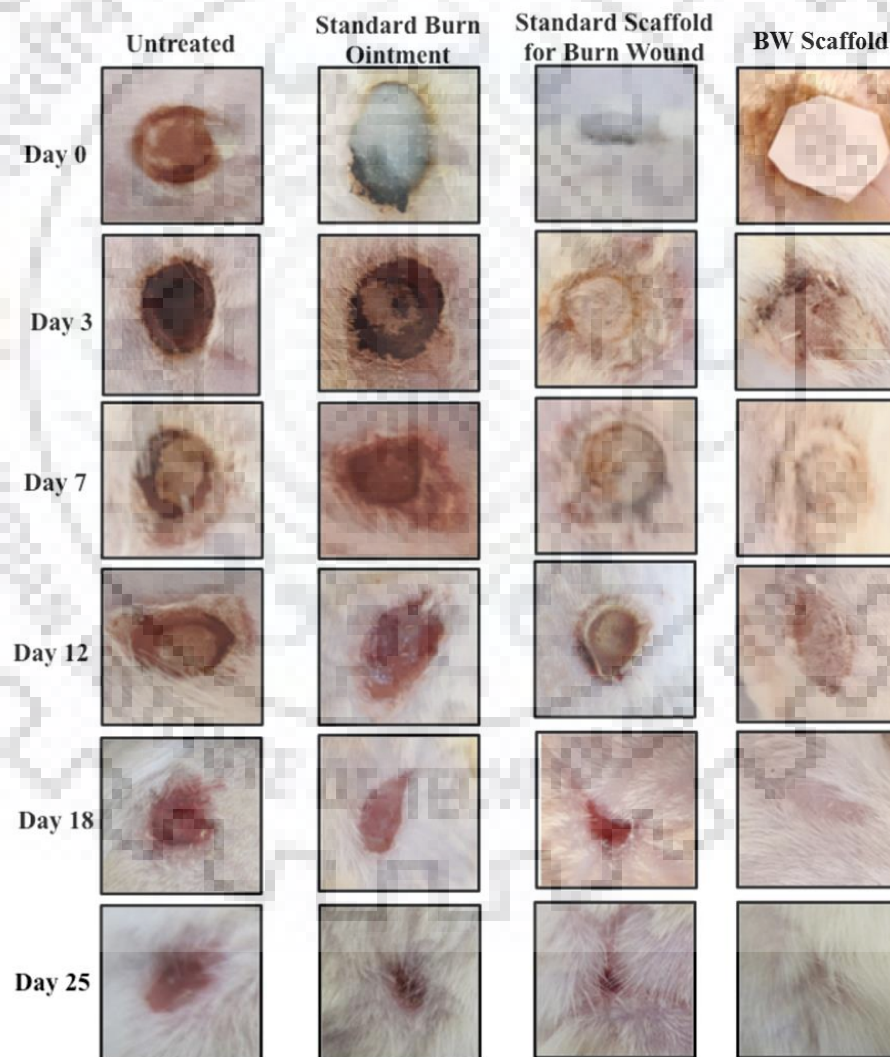

Figure 20: Tissue Regeneration Efficiency of the BW Scaffold

Optical images showing extent of wound closure at different time intervals over 25 days.
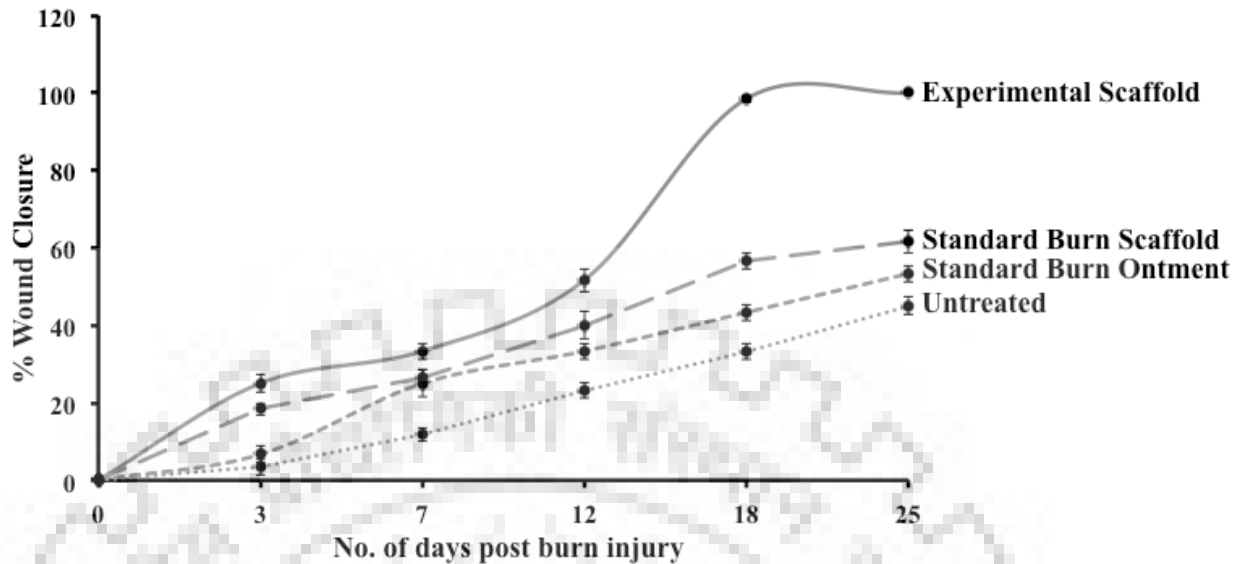
Figure 21: Efficiency of wound healing represented quantitatively as percent wound closure *versus* time plotted using the wound diameters measured over 25 days at time intervals corresponding to the optical images supplied in panel in **Figure 20**.

Pathophysiology of full thickness burn wound healing involves eschar/blister formation, inflammation, proliferation and finally, remodeling. While each of these steps are crucial for unaided natural healing, they have their own downsides so strong that a slight incoordination will be detrimental and can jeopardize the healing process altogether. For example, extensive eschar or blister formation with concomitant enhanced exudation can lead to higher chances of bacterial infection. However, the exudate itself has immense healing property. Similarly, inflammation is required for macrophage infiltration at the wound site for effective debridement and also accumulation of innate immune system at the site. But prolonged inflammation can lead to deregulated differentiation and excessive scarring. Inflammatory phase also leads to accumulation of Granular Tissue (GT) (a collection of stem cells, endothelial cells and keratinocytes), primarily to close the wound. GT also serves as the natural Extra Cellular Matrix (ECM) for the upcoming proliferation phase[35]. The proliferation stage sees the growth and differentiation of different cells. In the subsequent remodeling phase these cells migrate in response to durotaxis and paracrine activities to form defined tissue structure. Therefore, to follow the healing process at the

histological level, skin tissues were collected at every time point mentioned above till 12th day for analysis of tissue architecture through Hematoxyline Eosin (HE) staining. The imaged sections are compiled in **Figure 22**.

HE stained skin sections from untreated and standard groups did not have any discernable feature on 3rd day post injury. Those from standard scaffold group showed eschar formation (ES) by this time. However, skin section from the group treated with experimental scaffold did not show eschar formation. These tissues appeared to be rather advanced in the healing process as evident from discernable dermis (D), hypodermis (H), underlying skeletal muscle (SM), hair follicles (HF) and neovasculature (NV). Tissues from untreated group showed eschar formation by 7th day while those from standard group had granular tissue (GT) in addition to eschar by this time. In case of standard scaffold treated sections, a distinct zone of infiltrated cells (IC) was visible in addition to GT, indicating the healing process to have proceeded to the inflammation stage. ICs are essentially macrophages and neutrophils getting docked at the site of injury to facilitate debridement. This shows that the standard scaffold actually expedites the natural route of burn wound healing. By the 7th day, the tissue treated with experimental scaffold started showing mature blood vessels (BV) and neo-epidermis (NE) in addition to still regenerating layers of hypodermis and skeletal muscles beneath it. Hair follicles (HF) continue to flourish as earlier.

By 12th day, the untreated sections move into the inflammatory phase as evident from presence of granular tissue GT). The tissue section from the standard group showed presence of infiltrated cells (IC) indicating the onset of natural debridement. Inflammation continues in these tissues as indicated by the presence of GT. The sections from the standard scaffold group show a distinct zone of infiltrated cells (ICs) an indicative of acute inflammation. This assumption turned out to be true from the observation that puss was found while harvesting these tissues. In the long run, this might lead to scarring. By this time, the sections treated with experimental scaffold showed well-formed layers of skeletal muscles (SM) and hypodermis (H). Discontinuous epithelization or epidermis formation (E) was also seen **Figure 22**.
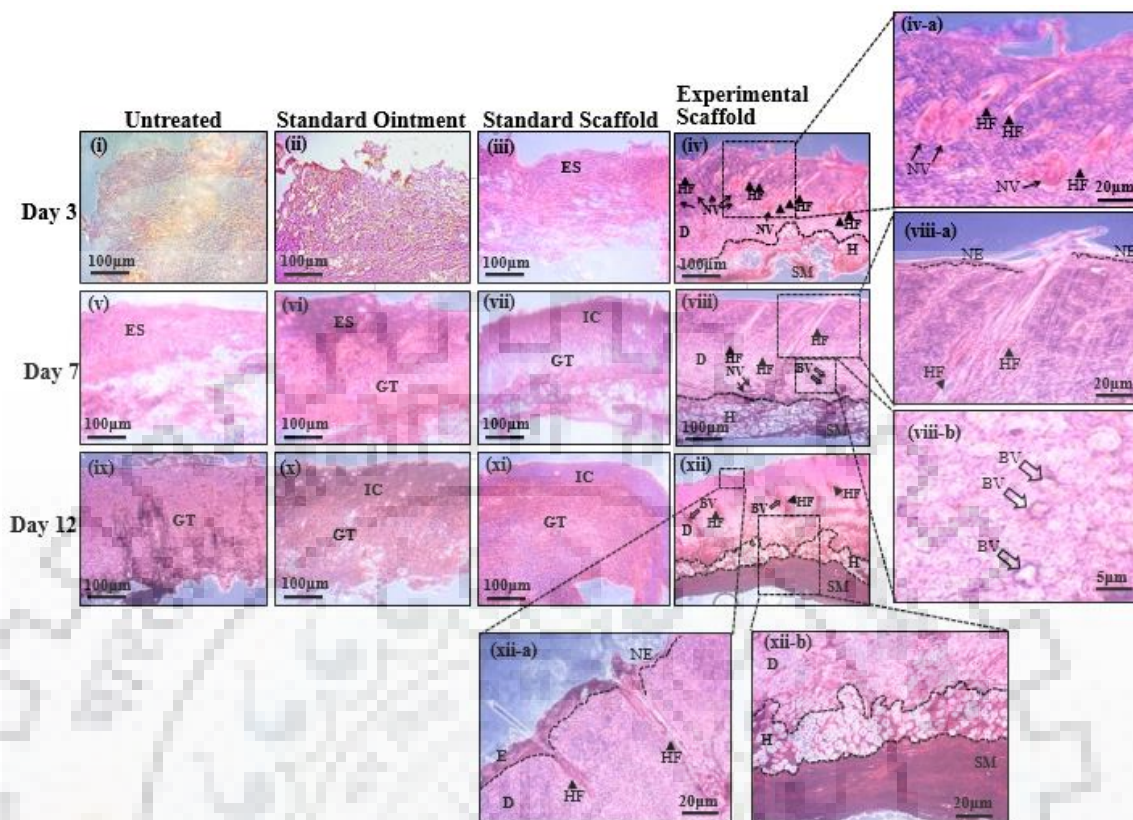
Figure 22: Representative images of Hematoxylin-Eosin (HE) stained transverse sections of skin tissues harvested after 3, 7 and 12 days of inflicting burn injury from untreated, standard burn ointment treated (Standard), commercially available burn wound scaffold treated (Standard Scaffold) and experimental scaffold treated (Experimental Scaffold) animals.

ES: eschar, **GT**: granulated tissue, **IC**: infiltrated cells, **E**: epidermis, **D**: dermis, **H**: hypodermis, **NV**: neovasculature (indicated with closed arrows), **BV**: mature blood vessels (indicated with open arrows), **HF**: hair follicles (indicated with arrowheads), **SM**: skeletal muscle.

Thermal injury leads to hepatic (liver) and nephric (kidney) toxicities[36,37]. Therefore, at regular intervals serum SGOT, SGPT, creatinine and urea levels were checked. SGOT and SGPT levels in all the groups were high by twelfth day post injury. However, no significant increase in serum creatinine and urea was observed around this time **(Figures 23 A-D)**. Absence of any significant difference in the **T**otal **L**eukocyte **C**ount (TLC) of the animals from experimental and control groups gave a clear idea of no

ensuing allergic reaction due to scaffold implantation, as visible increase in TLC would have suggested otherwise **(Figure 23E)**. All values were within the normal range of TLC for SD rats.
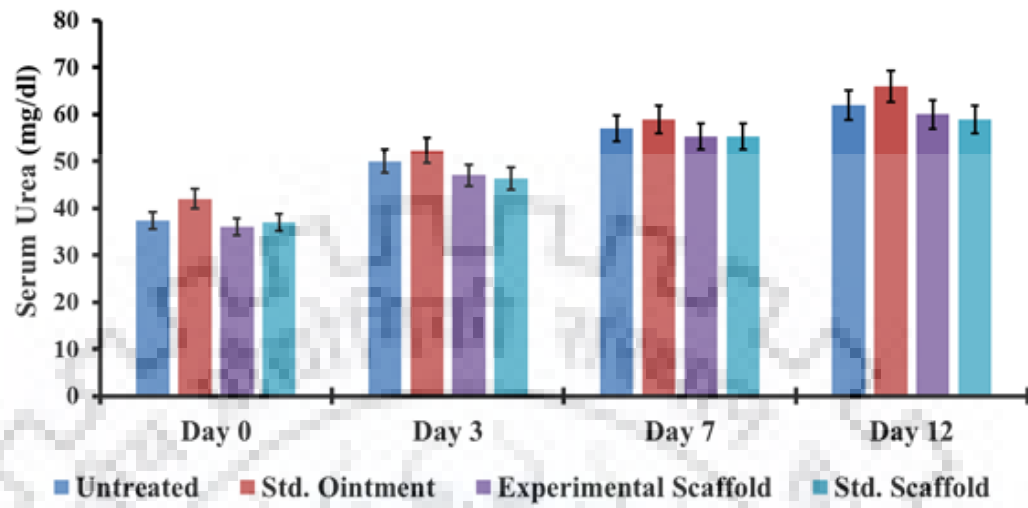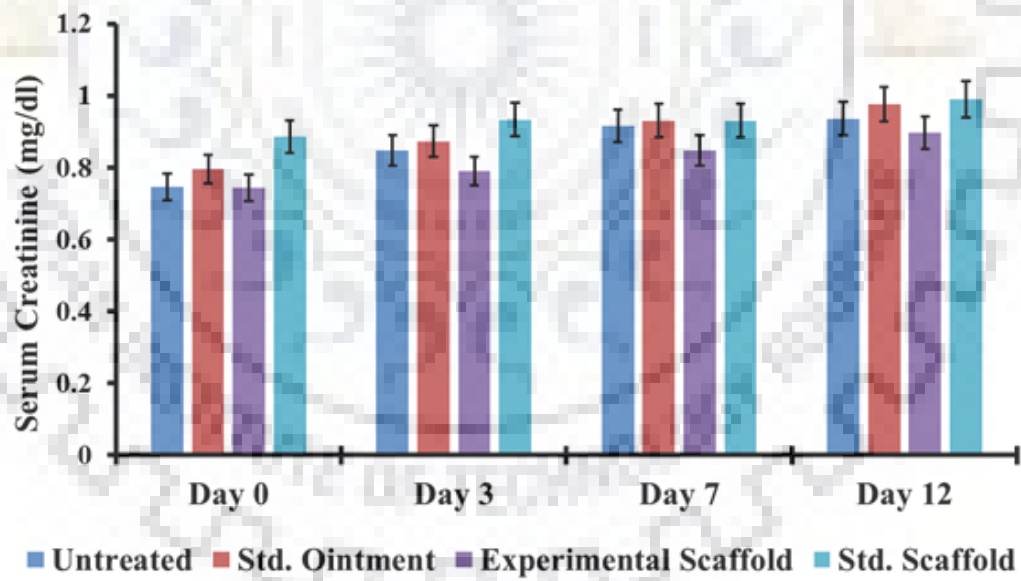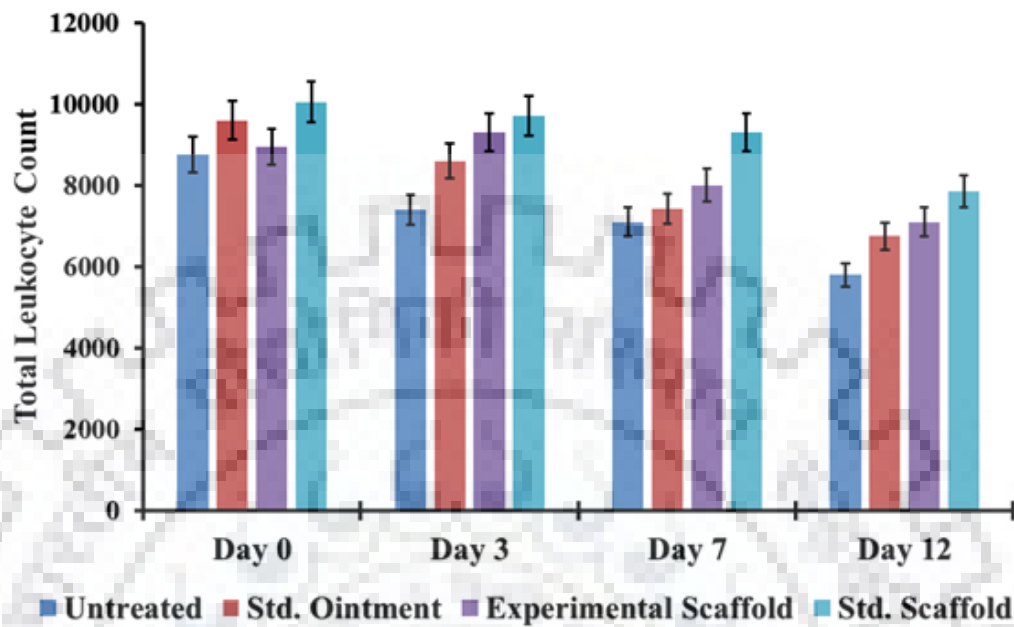
[A]
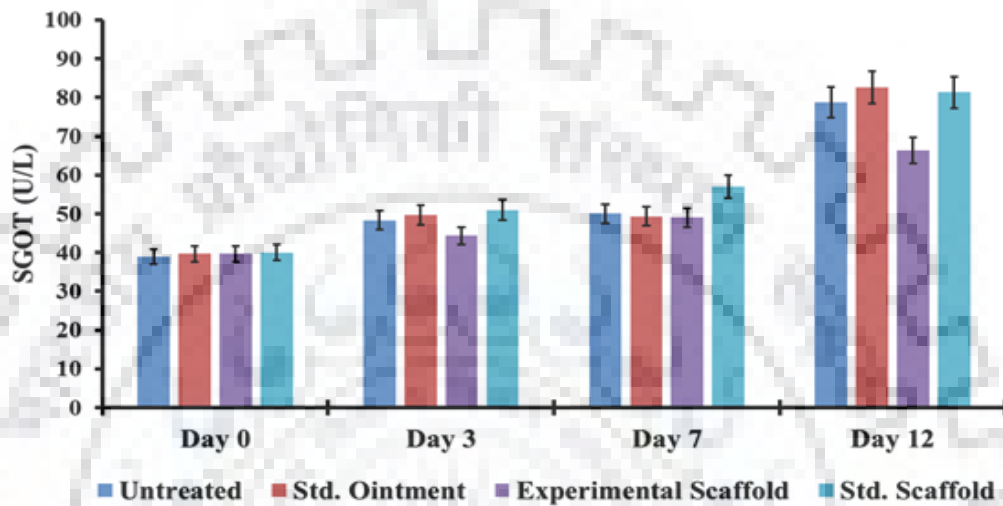
[B]
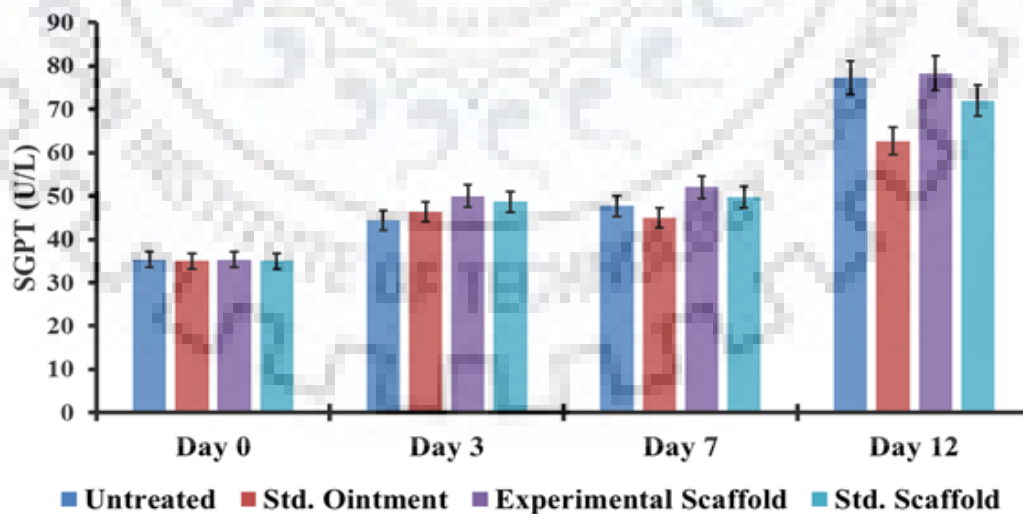
[C]

[D]

[E]

Figure 23: [A-E] Graphs showing the data from liver [A, B] and kidney [C, D] toxicity tests and Total Leukocyte Count (TLC) [E].

5. Discussion

Third-degree burn wound healing occurs in three phases, namely, reactive, reparative and reconstructive. During the reactive phase, the burn wound spreads out and is more vulnerable to infections and inflammation. The reparative phase, as the name suggests focuses on tissue repair primarily by engaging underlying stem cell repertoire in proliferation into different types of skin cells. The reconstructive phase ensures tissue building through the correct order of cell migration and differentiation. The composition of each layer of the proposed tri-layer BW scaffold was varied in conformance with their respective roles in burn wound healing.

Constructed here is a regenerative template that will protect burn wounds from contamination, bacterial infection, facilitate neovascularization, provide micro-niche for the regeneration of each layer of skin and ultimately get remodeled into the skin tissue. Thus, different layers of the invented tri-layer scaffold are fortified with bioactive agents and/or antibiotics. Microstructure and chemical compositions of the layers are engineered suitably to (a) mimic o*vera*ll spatial composition and mechanical property of skin ECM, and (b) ensure timely release of bioactive agents and antibiotics as par requirements of the healing process.

The topmost layer of the scaffold is least porous and hydrophobic to barricade against dirt, dust, and external sources of infection, prevent loss of moisture and facilitate re-epithelization. The microstructure and compactness of this layer is designed to resemble the extracellular matrix (ECM) that will support proliferation and differentiation of keratinocytes; the cells that constitute the epidermis. In addition, it will facilitate regeneration of the layers below epidermis through durotaxis. Therefore, this layer is composed of a hydrophobic polymer.

The middle layer is relatively less hydrophobic and more porous, providing the appropriate niche for proliferation and differentiation of dermal fibroblasts to ensure dermal regeneration. This layer is designed to facilitate the gradual release of antibiotic/s, bioactive anti-inflammatory agent and support dermal regeneration. The layer is fabricated

by the combination of biodegradable hydrophobic and hydrophilic polymers, along with antibiotics and bioactive agent. These polymer solutions have been deposited nano-fibers to modulate the release of antibiotic/s and anti-inflammatory agent, to tune in with the window of high bacterial infection and inflammation risks. This design was to avoid loss of antibiotics through initial diffusion. The antibiotics were selected based on the reported bacterial infection profiles of burn wounds. Although two antibiotics were used in this study, but a single one against both Gram-positive and Gram-negative bacteria will also suffice. Therefore, the choices of antibiotic that can be used are unlimited. The herbal bioactive agent included in the composition of the scaffold possesses anti-inflammatory activity. Besides, inflammation, this compound is potent as anti-viral and pro-angiogenic/vasculogenic agent; it soothes the wound, relieves pain, protects from viral infections and facilitates blood vessel formation[38,39].

The bottommost third layer is highly porous and extremely hydrophilic to resemble the ECM of hypodermis. It has high moisture retention capacity to support hypodermal regeneration. It is composed of deep freezed biodegradable natural polymer. This layer is also fortified with bioactive agent to provide a cooling effect to the burn wound, prevent acute inflammation and viral infection, and facilitate proliferation and immunomodulation via activation of macrophages[40].

The overall micro-architecture of the scaffold is designed to provide templates for simultaneous regeneration of all the layers of skin during the reconstruction phase of healing. Fabrication technique has been optimized to ensure adherence between the three layers of the scaffold. The scaffold incorporates all the features required to support the different stages of burn wound healing. The typical variation in the moisture absorption and retention capacities of the three layers of the scaffold plays a critical role in exudate management and providing moist care during wound healing, besides, providing other features mentioned earlier. The scaffold is composed of biodegradable components and will get resorbed and remodelled into skin tissue during wound healing.

6. Conclusion

The trilayer burn wound scaffold adds a new dimension to burn wound management. The architecture and composition ascertain micro management of needs of burn wounds. Exudate management and moisture provision during burn wound healing ensures protection form bacterial infections, as known to be rampant in case of third degree burn wounds. In addition, it supports simultaneous regeneration of all the layers of the skin without any need for post-healing removal of any component that fails to become a part of the regenerated skin. The design ensures remodeling of the scaffold into skin tissue with its complete integration into the body. Being equipped with antibiotics and bioactive agent, precisely aligned to meet the specific requirements of burn wound healing, this scaffold is capable of managing burn wounds at all levels of healing.

7. Future scope of work

Further work on the project includes:

1. Further *in vivo* confirmation on scar free burn wound healing potential of the scaffold on wounds of larger size.
2. Confirmation of the stability and shelf life of the scaffold.
3. Storage conditions and packaging requirements of the scaffold to be ascertained.

8. References

1.   World Health Organization (WHO). *Burns (Fact Sheet).* (2018). doi:10.1016/j.spinee.2013.09.052

2.   Evers, L. H., Bhavsar, D. & Mailänder, P. The biology of burn injury. *Exp. Dermatol.* **19**, 777–783 (2010).

3.   Robins, E. V. Burn shock. *Crit. Care Nurs. Clin. North Am.* **2**, 299–307 (1990).

4.   Roth, J. & Hughes, W. *The Essential Burn Unit Handbook.* (Quality Medical Publishing, St Louis, 2004). doi:10.1186/cc2990

5.   Tegos GP, Demidova TN, Arcila-Lopez D, Lee H, Wharton T, Gali H. Cationic Fullerenes Are Effective and Selective Antimicrobial Photosensitizers. *Chem. Biol.* **12**, 1127–1135 (2005).

6.   Barret-Nerín, J. P.0 & Herndon, D. N. *Principles and practice of burn surgery.* (Marcel Dekker, 2005).

7.   Neely AN, Brown RL, Clendening CE, Orloff MM, Gardner J, Greenhalgh DG. Proteolytic activity in human burn wounds. *Wound Repair Regen.* **5**, 302–309 (1997).

8.   Samonte VA, Goto M, Ravindranath TM, Fazal N, Holloway VM, Goyal A. Exacerbation of intestinal permeability in rats after a two-hit injury: burn and Enterococcus faecalis infection. *Crit. Care Med.* **32**, 2267–73 (2004).

9.   Queen, D., Evans, J., Gaylor, J., Courtney, J. & Reid, W. Burn wound dressings--a review. *Burn. Incl Therm Inj.* **13**, 218–28 (1987).

10.   Eldad, A., Burt, A., Clarke, J. & Gusterson, B. Cultured epithelium as a skin substitute. *Burn. Incl Therm Inj.* **13**, 173–80 (1987).

11.   Luca MD, Albanese E, Bondanza S, Megna M, Ugozzoli L, Molina F. Multicentre

experience in the treatment of burns with autologous and allogenic cultured epithelium, fresh or preserved in a frozen state. *Burns* **15**, 303–309 (1989).

12. Heimbach D, Luterman A, Burke J, Cram A, Herndon D, Hunt J. Artificial dermis for major burns. A multi-center randomized clinical trial. *Ann. Surg.* **208**, 313–20 (1988).

13. Atiyeh, B. S. & Costagliola, M. Cultured epithelial autograft (CEA) in burn treatment: Three decades later. *Burns* **33**, 405–413 (2007).

14. Bargues, L., Boyer, S., Leclerc, T., Duhamel, P. & Bey, E. Incidence et microbiologie des complications infectieuses lors d'utilisation de la peau artificielle Integra® chez le brûlé. *Ann. Chir. Plast. Esthet.* **54**, 533–539 (2009).

15. Arno, A. I. & Jeschke, M. G. The use of dermal substitutes in burn surgery: Acute phase. *Dermal Replace. Gen. Burn. Plast. Surg. Tissue Eng. Clin. Pract.* **9783709115**, 193–210 (2014).

16. Zhou P, Lessa N, Estrada DC, Severson EB, Lingala S, Zern MA. Decellularized liver matrix as a carrier for the transplantation of human fetal and primary hepatocytes in mice. *Liver Transplant.* **17**, 418–427 (2011).

17. Wainwright, D. J. Use of an acellular allograft dermal matrix (AlloDerm) in the management of full-thickness burns. *Burns* **21**, 243–248 (1995).

18. Austin, R. E., Merchant, N., Shahrokhi, S. E. & Jeschke, M. G. A Comparison of Biobrane[TM] and Cadaveric Allograft for Temporizing the Acute Burn Wound: Cost and Procedural Time. *Burns* **41**, 749–753 (2015).

19. Kokubo, T. & Takadama, H. How useful is SBF in predicting in vivo bone bioactivity? *Biomaterials* **27**, 2907–15 (2006).

20. Gamble, J. L. Chemical anatomy, physiology and pathology of extracellular fluid. in *Chemical anatomy, physiology and pathology of extracellular fluid.* 1–17 (Harvard University Press, 1967).

21. Gonzalez MR, Fleuchot B, Lauciello L, Jafari P, Applegate LA, Raffoul W. Effect of Human Burn Wound Exudate on Pseudomonas aeruginosa Virulence . *mSphere* **1**, 1–14 (2016).

22. Ulrich, D., Noah, E.-M., Heimburg, D. von & Pallua, N. TIMP-1, MMP-2, MMP-9, and PIIINP as serum markers for skin fibrosis in patients following severe burn trauma. *Plast. Reconstr. Surg.* **111**, (2003).

23. Neely AN, Brown RL, Clendening CE, Orloff MM, Gardner J, Greenhalgh DG. Original articles Proteolytic activity in human burn wounds. *Wound Repair Regen.* 302–309 (1997).

24. Drukała, J. Levels of plasma matrix metalloproteinases (MMP-2 and MMP-9) in response to INTEGRA® dermal regeneration template implantation. *Med. Sci. Monit.* **20**, 91–96 (2014).

25. Hästbacka J, Fredén F, Hult M, Bergquist M, Wilkman E, Vuola J. Matrix metalloproteinases -8 and -9 and tissue inhibitor of metalloproteinase-1 in burn patients. A prospective observational study. *PLoS One* **10**, 1–18 (2015).

26. Rivero HG, Lee JO, Herndon DN, Mecott GA, Kulp GA, Kraft R. The role of acute pancreatitis in pediatric burn patients. *Burns* **37**, 82–85 (2011).

27. Colleen, R., L, S. R., A, S. D., Andrew, W. & Thompkins Ronald G. Complications of pancreatitis in severely burned patients. *Ann. Surg.* 8000 (1995).

28. Abu-Shandi & Khalid, H. Determination of vancomycin in human plasma using high-performance liquid chromatography with fluorescence detection. *Anal. Bioanal. Chem.* **395**, 527–532 (2009).

29. Qi L, Knapton EK, Zhang X, Zhang T, Gu C, Zhao Y. Pre-culture Sudan Black B treatment suppresses autofluorescence signals emitted from polymer tissue scaffolds. *Sci. Rep.* **7**, 1–12 (2017).

30. Cai EZ, Ang CH, Raju A, Tan KB, Hing ECH, Loo Y. Creation of consistent burn

wounds: A rat model. *Arch. Plast. Surg.* **41**, 317–324 (2014).

31. Pal P, Dadhich P, Srivas PK, Das B, Maulik D, Dhara S. Bilayered nanofibrous 3D hierarchy as skin rudiment by emulsion electrospinning for burn wound management. *Biomater. Sci.* **5**, 1786–1799 (2017).

32. Gallagher AJ, Ní Anniadh A, Bruyere K, Otténio M, Xie H, Gilchris MD. Dynamic Tensile Properties of Human Skin. *IRCOBI Conf.* 494–502 (2012).

33. Kalra, A. & Lowe, A. Mechanical Behaviour of Skin: A Review. *J. Mater. Sci. Eng.* **5**, (2016).

34. Szaniszlo, B., Iuga, C. & Bojiţă, M. Indirect Determination of Gentamicin by Derivative Spectrophotometry. *Acta Medica Marisiensis* **84**, 398 (2011).

35. Ridiandries A, Tan J, Bursill C, Ridiandries A, Tan JTM, Bursill CA. The Role of Chemokines in Wound Healing. *Int. J. Mol. Sci.* **19**, 3217 (2018).

36. Adiga, U. & Adiga, S. Biochemical Changes in Burns. *Int. J. Res. Stud. Biosci.* **3**, 88–91 (2015).

37. Jeschke, M. G. The Hepatic Response to Thermal Injury: Is the Liver Important for Postburn Outcomes? *Mol. Med.* **15**, 337–351 (2009).

38. Xing W, Guo W, Zou CH, Fu TT, Li XY, Zhu M. Acemannan accelerates cell proliferation and skin wound healing through AKT/mTOR signaling pathway. *J. Dermatol. Sci.* **79**, 101–109 (2014).

39. Qiu, Z., Jones, K., Wylie, M., Jia, Q. & Orndorff, S. Modified Aloe barbadensis polysaccharide with immunoregulatory activity. *Planta Med.* **66**, 152–156 (2000).

40. Maharjan H., R. & Nampoothiri P., L. Evaluation of biological properties and clinical effectiveness of Aloe vera: A systematic review. *J. Tradit. Complement. Med.* **5**, 21–26 (2015).